The Company of **Biologists**

RESEARCH ARTICLE

The role of icIL-1RA in keratinocyte senescence and development of the senescence-associated secretory phenotype

Sven E. Niklander[1,2], Hannah L. Crane[1], Lav Darda[1], Daniel W. Lambert[1] and Keith D. Hunter[1,3,*]

ABSTRACT

There is compelling evidence that senescent cells, through the senescence-associated secretory phenotype (SASP), can promote malignant transformation and invasion. Interleukin-1 (IL-1) is a key mediator of this cytokine network, but the control of its activity in the senescence programme has not been elucidated. IL-1 signalling is regulated by IL-1RA, which has four variants. Here, we show that expression of intracellular IL-1RA type 1 (icIL-1RA1), which competitively inhibits binding of IL-1 to its receptor, is progressively lost during oral carcinogenesis *ex vivo* and that the pattern of expression is associated with keratinocyte replicative fate *in vitro*. We demonstrate that icIL-1RA1 is an important regulator of the SASP in mortal cells, as CRISPR/Cas9-mediated icIL-1RA1 knockdown in normal and mortal dysplastic oral keratinocytes is followed by increased IL-6 and IL-8 secretion, and rapid senescence following release from RhoA-activated kinase inhibition. Thus, we suggest that downregulation of icIL-1RA1 in early stages of the carcinogenesis process can enable the development of a premature and deregulated SASP, creating a pro-inflammatory state in which cancer is more likely to arise.

KEY WORDS: Head and neck cancer, Interleukin 1 receptor antagonist, IL-1RA, Senescence, SASP

INTRODUCTION

The Interleukin-1 (IL-1) receptor antagonist (IL-1RA) is an important regulator of IL-1 signalling in health and disease. IL-1RA acts as the main IL-1 inhibitor and has no agonist actions (Kurzrock et al., 2019), as it is a competitive antagonist of the IL-1 agonist receptor (IL-1R1), preventing IL-1 binding and the activation of downstream pathways (Hannum et al., 1990). IL-1RA is also able to inhibit the NF-κB and p38 MAPK transduction pathways in a non-IL-1R1-dependent manner (Garat and Arend, 2003). IL-1RA is coded by the *IL1RN* gene located at 2q14 (Eisenberg et al., 1990) and encodes four IL-1RA protein variants, one secreted (sIL-1RA) and three intracellular forms (icIL-1RA1-3), by alternate splicing (Haskill et al., 1991). sIL-1RA is a 17 kDa protein secreted by monocytes and neutrophils (Malyak et al., 1998a). The intracellular variants lack a leader peptide thus cannot be secreted (Haskill et al., 1991). icIL-1RA1 is the main

intracellular variant with a molecular weight of 18 kDa, and is mainly expressed in keratinocytes and other epithelial cells, monocytes, tissue macrophages, fibroblasts and endothelial cells. icIL-1RA2 protein has never been found in human cells (Arend, 2002). icIL-1RA3 has been found in monocytes, neutrophils and macrophages (Malyak et al., 1998b), but has fivefold less affinity to IL-1R1 than the other forms and has not been reported in keratinocytes (Malyak et al., 1998a,b; Weissbach et al., 1998).

In senescent cells, IL-1 signalling is closely associated with the development of the senescence-associated secretory phenotype (SASP) (Lau et al., 2019), a secretory state characterized by the production of more than 40 factors involved in intercellular signalling (Davalos et al., 2010). This includes a number of pro-inflammatory cytokines, including IL-6 and IL-8, molecules known to induce epithelial-to-mesenchymal transition and invasion of pre-malignant cells (Malaquin et al., 2013; Coppé et al., 2008; Ortiz-Montero et al., 2017; Lau et al., 2019). Thus senescence, although being a potent suppressor of malignancy in mutated pre-malignant cells, is also considered to participate in the tumour-promoting neoplastic environment (Campisi, 2005), as senescent cells are found in pre-malignant lesions *in vivo* (Guo et al., 2019), including those of the oral cavity (Natarajan et al., 2003). IL-1 signalling is important for the development of a microenvironment able to promote cancer development (Orjalo et al., 2009; Lau et al., 2019), as it regulates IL-6 and IL-8 (also known as CXCL8) via NF-κB activation (Wolf et al., 2001; Orjalo et al., 2009; Rovillain et al., 2011). Reduction in the levels of its natural antagonist IL-1RA has been related to tumour growth, invasion and metastasis (La et al., 2001; Lewis et al., 2006), and could allow a de-regulation of the SASP (Acosta et al., 2013).

A number of transcriptomic studies have independently found *IL-1RN* to be downregulated in mucosal head and neck cancers (HNC) when compared to matched normal oral mucosa (Alevizos et al., 2001; Choi and Chen, 2005; Cromer et al., 2004; Leethanakul et al., 2000; Schmalbach et al., 2004; Whipple et al., 2004; Lallemant et al., 2009; Koike et al., 2005). Recently, Shiiba et al. (2015) reported total IL-1RA protein expression was progressively downregulated through oral dysplasia to oral squamous cell carcinoma (OSCC) (Shiiba et al., 2015), but its consequences are poorly understood. HNC constitute the eighth most common cancer worldwide and causes significant morbidity and mortality, with a 5-year survival rate of ∼50% (Marur and Forastiere, 2016). Oral cancer arises in many cases from oral potentially malignant disorders (OPMDs), which can present clinically as leukoplakias and erythroplakias (Villa et al., 2019). No treatment has been proven to successfully reduce malignant transformation of OPMDs (Lodi et al., 2016). Thus, it is important to identify the mechanisms involved in oral malignant transformation that could be pharmacologically targeted.

As IL-1RA downregulation is progressively observed through OD to OSCC, we examined the contribution of IL-1RA to the

[1]Unit of Oral and Maxillofacial Medicine, Pathology and Surgery, University of Sheffield, Sheffield S10 2TA, UK. [2]Departamento de Cirugia y Patologia Oral, Facultad de Odontologia, Universidad Andres Bello, 2520000 Viña del Mar, Chile. [3]Oral Biology and Pathology, University of Pretoria, Pretoria, South Africa.

*Author for correspondence (k.hunter@sheffield.ac.uk)

S.E.N., 0000-0003-1858-3091; H.L.C., 0000-0003-1129-0413; L.D., 0000-0003-4709-1707; K.D.H., 0000-0002-7873-0877

development of senescence and a pro-tumourigenic SASP (which has not been characterized in oral keratinocytes), which may be an important component of the malignant transformation process.

RESULTS

Intracellular IL-1RA expression is lost during carcinogenesis of oral keratinocytes

To assess *IL1RN* expression during oral carcinogenesis, *IL1RN* transcript levels were analysed in a panel of mortal normal oral keratinocytes (NOKs; NOK805 and NOK829), immortalized normal oral keratinocytes (iNOKs: FNB6, OKF4 and OKF6), mortal and immortal dysplastic oral keratinocytes (OD: D6, D25 and D19, and D20, respectively) and malignant oral keratinocytes (OSCC: B16 and B22). We observed a progressive decrease in *IL1RN* transcript levels in OD and OSCC cell lines compared to NOKs (Fig. 1A and Fig. S1A for individual cell expression that includes iNOKs). Total IL-1RA (tIL-1RA) protein levels were concordant with the qPCR data, showing a decrease in tIL-1RA protein in OD and OSCC cell lines compared to NOKs (Fig. 1B). The decrease in tIL-1RA protein levels in OD and OSCC cells can be attributed to a decrease in mRNA levels of the intracellular variant (*icIL-1RN*; Fig. 1C). Despite expression levels of *sIL-1RN* seemingly decreasing in OD and OSCC cell lines compared to NOKs, no significant differences were observed (Fig. 1D). The dominant isoform expressed in oral keratinocytes is *icIL-1RN* transcript variant 3, which encodes icIL-1RA type I (icIL-1RA1) (Fig. S1B). None of the immortal OD and OSCC cells showed any tIL-1RA expression (D19 and D20, and B16 and B22, respectively), whereas tIL-1RA was readily detected in FNB6 (Fig. 1B,E), in keeping with the transcript abundance. tIL-1RA was located diffusely across the cytoplasm and is present in the nucleus of FNB6 (Fig. 1F). Immunohistochemical assessment of tIL-1RA expression in a panel of five normal oral mucosa, nine OD and ten OSCC patient tissue samples showed a reduction in expression in agreement with our *in vitro* data, with robust expression of tIL-1RA in normal oral epithelium and progressive loss of expression in OD and OSCC (Fig. 1G,H).

In order to assess whether OD and OSCC cells still retain the capability to upregulate IL1-RA under inflammatory stimuli, OD and OSCC cell lines with undetectable IL-1RA protein were treated with recombinant IL-1α or IL-1β (10 ng/ml). Neither IL-1α nor IL-1β affected tIL-1RA and *icIL-1RN* mRNA levels in OD and OSCC cell lines (Fig. S1C-F), but IL-1β did induce IL-6 and IL-8 secretion, indicative of functional signalling (Fig. S1G). Recombinant IL-1α significantly increased *icIL-1RN* mRNA levels in FNB6 cells, confirming also that the recombinant protein was functional (Fig. S1H). tIL-1RA protein was not detected in any of the OD and OSCC cell lines before or after IL-1α or IL-1β stimulation (Fig. S1C-F). In order to assess whether another endogenous IL-1 inhibitor might be replacing this function in low-IL-1RA-expressing cells, we analysed IL-1R2 expression, a decoy IL-1 receptor that acts as a molecular trap, inactivating IL-1 (Colotta et al., 1994). No difference in IL-1R2 mRNA levels between immortal NOK, immortal OD and OSCC cell lines was observed (Fig. S1I), and IL-1R2 transcript levels did not change after IL-1 stimulation in any of the tested cell lines (Fig. S1J). These data suggest that *IL1RN* downregulation in OD and OSCC cells is not reversible upon IL-1 stimulation and is not being compensated for by an increase in IL-1R2.

Immortal oral keratinocytes consistently expressed lower *IL1RN* transcript levels than their mortal counterparts (Fig. S1A; Fig. 1I-K). Similarly, tIL-1RA protein levels decreased in immortal cells

(Fig. 1B). These data indicate a deregulation of the IL-1 inhibition system during oral carcinogenesis, which can occur at precancerous/dysplasia stages and which is more closely associated with the acquisition of replicative immortality than the stage of disease development (McGregor et al., 2002).

IL-1R1 is upregulated in oral dysplastic and oral cancer cell lines compared to NOKs

To further characterize the regulation of IL-1 signalling during the oral carcinogenesis process, we analysed the expression of IL-1R1. IL-1R1 transcript levels were significantly upregulated in immortal and mortal OD compared to NOKs and iNOKs (Fig. 2A). As with *IL1RN*, IL-1R1 expression decreases in immortal cells compared to their mortal counterpart (Fig. 2B). Immunofluorescence showed endogenous expression of IL-1R1 in immortal OD and OSCC cells, but showed no expression in iNOKs (Fig. 2C). IL-1R1 upregulation in OD and OSCC corresponded with higher endogenous levels of IL-1α protein (Fig. 2D). In B16 (Fig. 2E) and D20 (Fig. 2F) cells, IL-1R1 was distributed diffusely across the cell membrane, but also inside or on the nucleus. To study the pattern of IL-1R1 expression under IL-1 stimulation, we treated B16 and D20 cells with recombinant IL-1α and recombinant IL-1β. IL-1α did not change IL-1R1 expression or localization, but treatment with IL-1β did increase IL-1R1 nuclear localization in both B16 and D20 cell lines (Fig. 2E,F). IL-1R1 nuclear expression increased significantly after IL-1β treatment in B16 cells (*P*=0.0026) (Fig. 2G).

icIL-1RA1 regulates IL-6 and IL-8 secretion in mortal oral keratinocytes

Next, we knocked down (KD) icIL-1RA1 in primary normal and dysplastic oral keratinocytes (NOK805 and D6, respectively) using CRISPR/Cas9. As IL-1α is an important regulator of IL-6 and IL-8, we aimed to determine whether IL-1RA downregulation may favour oral cancer development by resulting in the overexpression of these cytokines. tIL-1RA protein levels in NOK805 KD (Fig. 3A) and D6 KD (Fig. 3B) cells were significantly lower than in their wild-type (WT) counterpart. A low level of expression was retained, suggesting a heterogeneous population (Fig. S2A-D). Owing to limitations in the replicative lifespan (8-10 passages), both cell types (KD and WT NOK805 and D6 cells) were maintained in culture with the RhoA-activated kinase (ROCK) inhibitor (Y-27632), previously reported to delay the onset of senescence in primary keratinocytes (Chapman et al., 2014). When using the CRISPR-modified and control cells, Y-27632 was removed from the culture medium and senescence-associated β-galactosidase activity was assessed. This was carried out to confirm that the edited cells did not senesce immediately after removing Y-27632 (Fig. S3A,B) due to the drug-induced lifespan extension, and that the observed changes were attributed to icIL-1RA1 KD and not to the induction of senescence.

When comparing KD and WT cells, we found a significant increase in IL-6 and IL-8 secretion in both NOK805 (Fig. 3C,D) and D6 (Fig. 3E,F) KD cells compared to WT controls. To assess whether these changes could be attributed to an increase in NF-κB pathway activation due to a lack of IL-1 inhibition, we analysed the activation NF-κB pathway by measuring the phosphorylation of p65. p65 phosphorylation increased in both NOK805 KD (Fig. 3G) and D6 KD (Fig. 3H) compared to WT cells, with no changes in total p65 levels. These data suggest that alterations in icIL-1RA1 expression result in changes in IL-6 and IL-8 levels, which may be mediated by alterations in the activity of the NF-kB pathway.
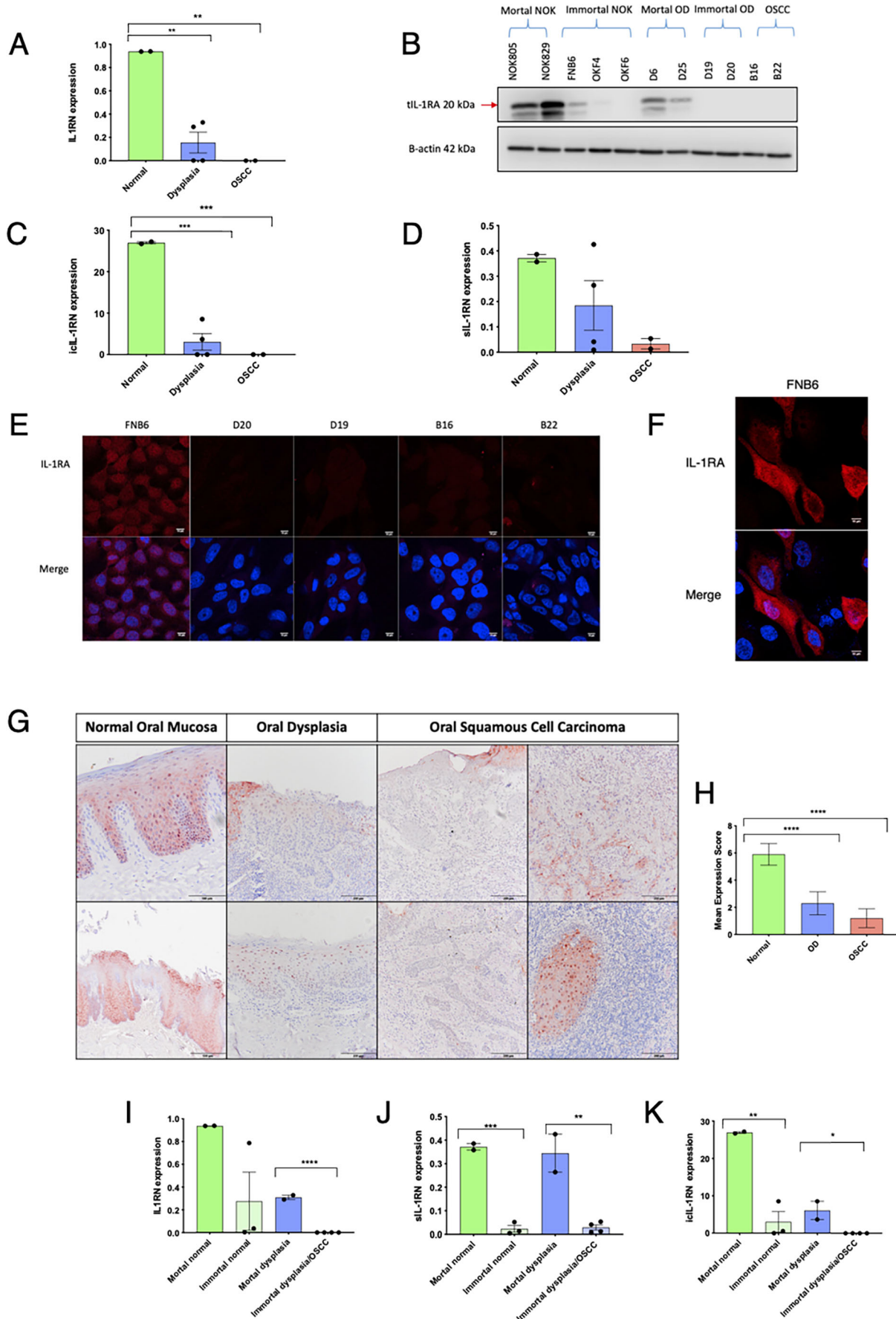
Fig. 1. See next page for legend.

Fig. 1. IL-1RA is downregulated during oral carcinogenesis *in vitro* and *in vivo*. (A,C,D) Data obtained from two primary NOK cell cultures (NOK805 and NOK829), four dysplastic cell cultures (D6, D25, D19 and D20) and two oral cancer cell lines (B16 and B22) were clustered together into three groups: normal, dysplasia and OSCC, respectively. Graphs show IL1RN (A), icIL-1RN (C) and sIL-1RN (D) mRNA expression as fold change. (B) Immunoblotting of tIL-1RA protein expression in the different cell cultures. (E,F) Representative confocal images of IL-1RA in different cell lines (E). IL-1RA localization in one immortal NOK cell line (F). Scale bars: 10 µm. (G,H) Representative immunohistochemical pictures of IL-1RA expression in patient tissue samples (G). IL-1RA is downregulated in OD and OSCC samples, but occasionally some OSCCs retain some IL-1RA expression. Scale bars: 100 µm; normal oral mucosa lower panel, 200 µm. Mean expression scores of IL-1RA expression in the different groups (H). (I-K) IL-1RN (I), icIL-1RN (J) and sIL-1RN (K) mRNA expression in the different cell cultures according to their mortality state in culture. Expression is presented as fold change relative to the reference gene. Data are mean±s.e.m. (*N*=3 independent experiments, and *n*=3 technical replicates). One-way ANOVA with multiple comparisons (A,C,D) or an unpaired two-tailed *t*-test (H-K) was used to calculate the exact *P* value (*$P<0.05$; **$P<0.005$; ***$P<0.0007$; ****$P<0.00001$).

icIL-1RA1 does not modify proliferation or migration of immortal pre-malignant and malignant oral keratinocytes

To assess whether re-expression of icIL-1RA1 in cells in which IL-1RA expression has been lost could affect cell behaviour, we transfected two immortal cell lines with undetectable levels of IL-1RA protein (B16 and D20) with a vector encoding icIL-1RA1 (Fig. 4A). Transfection efficiency was above 50% for both cell types (Fig. 4B). Transfection of icIL-1RA1 did not affect proliferation (Fig. 4C,D) or alter cell migration (Fig. 4E,F) in either cell line. In B16 icIL-1RA1-transfected cells, a decrease in IL-8 secretion (but not Il-6) was observed, but only when cells were stimulated with IL-1β. No changes in D20 icIL-1RA1 transfected cells were observed (Fig. 4G-J).

IL-1RA expression decreases during replicative senescence

Replicative senescence is an important anti-tumour response, which paradoxically can also promote tumour formation if not tightly regulated. IL-1α has been identified as a key factor in the regulation of senescence and the SASP (Wiggins et al., 2019). Thus, we hypothesized that a decrease in tIL-1RA could switch the senescence response from preventing tumour formation, to promoting cancer development, by allowing an overexpression of inflammatory factors known to have pro-tumourigenic effects, such as IL-1, IL-6 and IL-8 (Acosta et al., 2013). In both normal (Fig. S4A) and dysplastic (Fig. S4B) oral keratinocytes, p16Ink4a, p21$^{Waf1/Cip1}$ and SA-β-galactosidase activity (Fig. S4C) increased gradually with passage. Phosphorylation of H2AX (γH2AX) also increased significantly with time in culture of all cell types (Fig. S4D-G).

tIL-1RA protein expression decreased gradually with the acquisition of replicative senescence in both normal (Fig. 5A) and dysplastic cells (Fig. 5C). icIL-1RN transcript levels also decreased significantly during aging in all of the cell cultures (Fig. 5B,D). We then analysed the expression of commonly expressed SASP factors known to be able to promote tumour formation: IL-1β, IL-1α, IL-6 and IL-8. Secretion of IL-1β increased in both senescent NOK (Fig. 5E) and OD cell cultures (Fig. 5F), and IL-1α protein expression increased in all senescent cell cultures apart from D6 cells (Fig. 5G,H). Secretion of IL-6 and IL-8 (Fig. 5I-L), and IL-6 and IL-8 mRNA transcript levels (Fig. S5A,B) increased gradually in all of the cell types during senescence. Interestingly, senescent ODs secreted more IL-6 and IL-8 than both senescent NOKs (Fig. S4H) (apart from secreted IL-8 from NOK805 cells), suggesting an enhancement of the SASP in dysplastic cells.

The cGAS–STING pathway is activated during oral keratinocyte senescence

Senescent normal and dysplastic oral keratinocytes developed cytoplasmic chromatin fragments (CCF) (Fig. 6A; Fig. S5C), probably as a consequence of a weakened nuclear membrane caused by a decrease in Lamin B1 expression (Fig. 6B). CCF have been reported to regulate senescence and the SASP by activating the cGAS–STING pathway (Dou et al., 2017; Glück et al., 2017). Thus, we decided to assess activation of the cGAS–STING pathway during oral keratinocyte senescence. One of the downstream products of the cGAS–STING pathway is IFN-β. IFN-β mRNA transcript levels increased significantly in all cell types, except NOK805 cells, upon senescence (Fig. 6C). To examine activation of the cGAS–STING pathway, we treated senescent dysplastic cells (D6) with the cGAS inhibitor RU.521 (Vincent et al., 2017), and assessed changes in SASP components and NF-κB activation. Cell viability was assessed with Trypan Blue staining. RU.521 was not toxic at any of the concentrations used (Fig. 6D). IL-6 secretion was significantly reduced by treating senescent cells with 10 µg/ml and 20 µg/ml of RU.521 (Fig. 6E), but not with lower doses. Contrary to this, treatment with RU.521 had no effect on secreted IL-1β (Fig. 6F) and IL-8 (Fig. 6G). In accordance with the decrease in secreted IL-6, treatment with 10 µg/ml or 20 µg/ml of RU.521 also reduced phosphorylation of p65 (Fig. 6H). A decrease in IL-1RA protein expression was also observed (Fig. 6H), which may be a consequence of the decrease in p65 phosphorylation.

icIL-1RA1 regulates the onset of senescence and the development of the SASP

In order to determine the specific role of icIL-1RA1 during senescence, and the regulation of the SASP, we removed Y-27632 from WT and icIL-1RA1 KD D6 cells, and expanded them until replicative senescence was achieved. Both KD and WT cells were at the same passage number when Y-27632 was removed from culture medium. D6 KD cells senesced prematurely compared to D6 WT cells (Fig. 7A). On average, 87.5% of the D6 KD cells stained positive for SA-β-gal after one passage, compared with 27.9% of the D6 WT at the same PDs (Fig. 7A,B). This corresponded with the cessation of cell growth observed in the KD cells, which could not be passaged further. Contrary to this, the D6 control cells were passaged one more time before achieving a SA-β-gal expression of 81% (Fig. 7A,B). A statistically significant difference in population doublings before senescence was observed when comparing KD and WT cells ($P<0.0001$); icIL-1RA1 KD cells doubled their population 0.7 times before senescing, whereas the WT cells doubled 2.4 times (Fig. 7C).

Both D6 KD and WT cells showed an increase in p16^{Ink4a} protein expression following the removal of Y-27632, with higher p16^{Ink4a} expression in WT than KD senescent cells (Fig. 7D). As shown previously, knockout of icIL-1RA1 significantly increased phosphorylation of p65 (Fig. 3G,H); this also further increased significantly in the senescent WT and KD cells (Fig. 7E). Nevertheless, once the cells had senesced, both cell groups (KD and WT) exhibited a similar level of p65 phosphorylation. D6 KD cells expressed lower IL-1RA protein levels than D6 WT cells (this as a consequence of gene editing), but when cells had senesced, IL-1RA protein expression of WT cells decreased significantly, similar to the amounts observed in KD cells (Fig. 7F). Once cells had senesced, both WT and KD groups experienced a significant increase in secreted IL-6 and IL-8. No difference in IL-6 and IL-8 secretion was observed between senescent WT and KD D6 cells (Fig. 7G,H). Altogether, these findings suggest that in oral
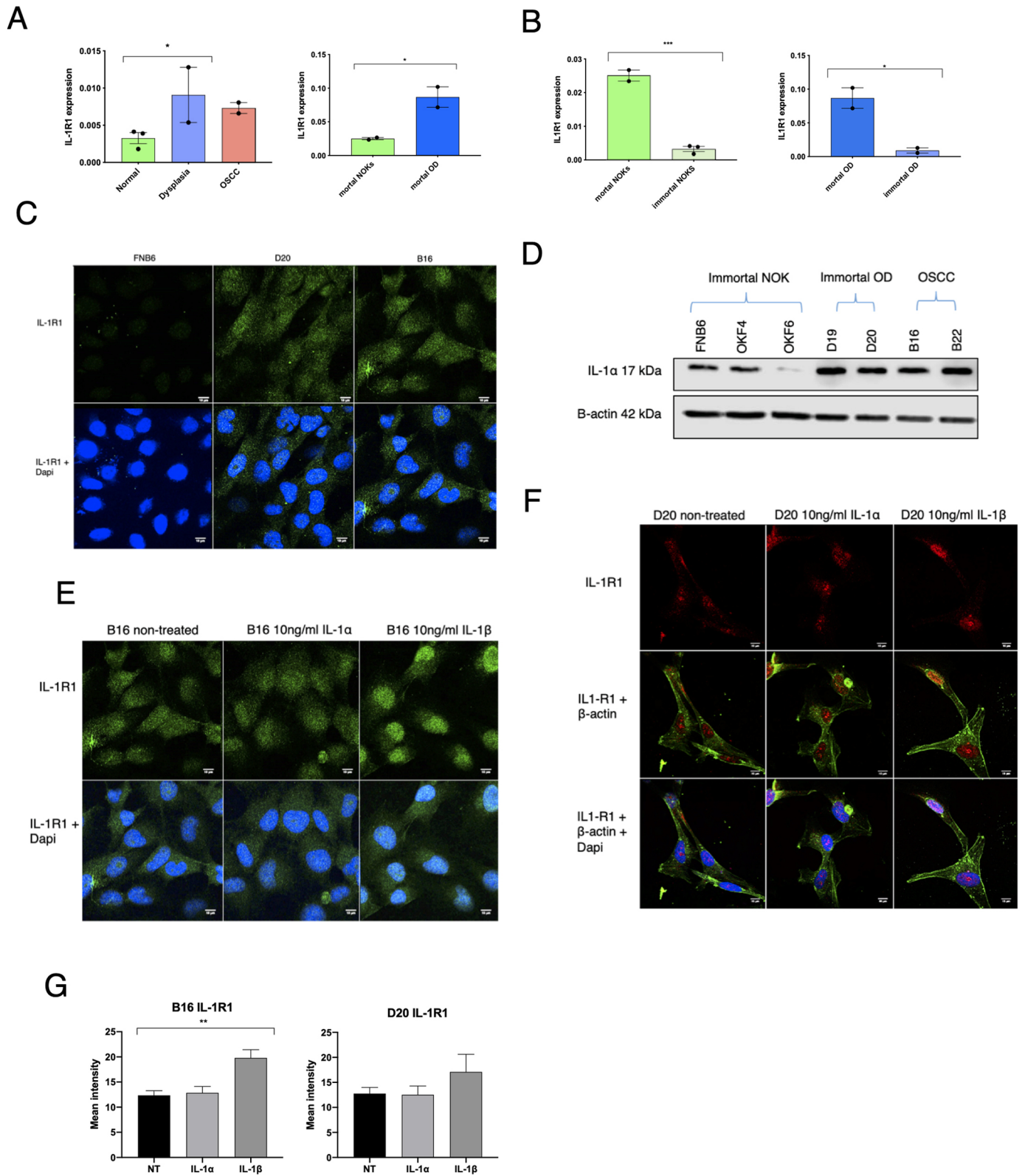
Fig. 2. IL-1R1 is upregulated in OD and oral cancer cell lines. (A) IL-1R1 mRNA expression in immortal NOKs (FNB6, OKF4 and OKF6), immortal OD (D19 and D20) and OSCC (B16 and B22) cell lines, and in mortal normal and dysplastic keratinocytes. Expression is presented as fold change relative to the reference gene. (B) IL-1R1 mRNA expression in the different cell cultures according to their mortality state in culture. Expression is presented as fold change relative to the reference gene. (C) Representative confocal images of IL-1R1 expression in FNB6, D20 and B16 cell lines. (D) Immunoblotting of IL-1α protein expression in the different immortal cell lines. (E,F) Representative confocal images of IL-1R1 expression after stimulation with rIL-1α and rIL-1β in OSCC (E) and OD (F) cells. (G) Quantification of IL-1R1 nuclear expression after stimulation with rIL-1α and rIL-1β in B16 and D20 cells. Data are mean±s.e.m. One-way ANOVA with multiple comparisons (A,G) or an unpaired two-tailed *t*-test (B) was used to calculate the exact *P* value (in A and B, *N*=3 independent experiments and *n*=3 technical replicates, and in G, *N*=2 independent experiments; *P*<0.05; **P*<0.005; ***P*<0.0009). Scale bars: 10 µm.
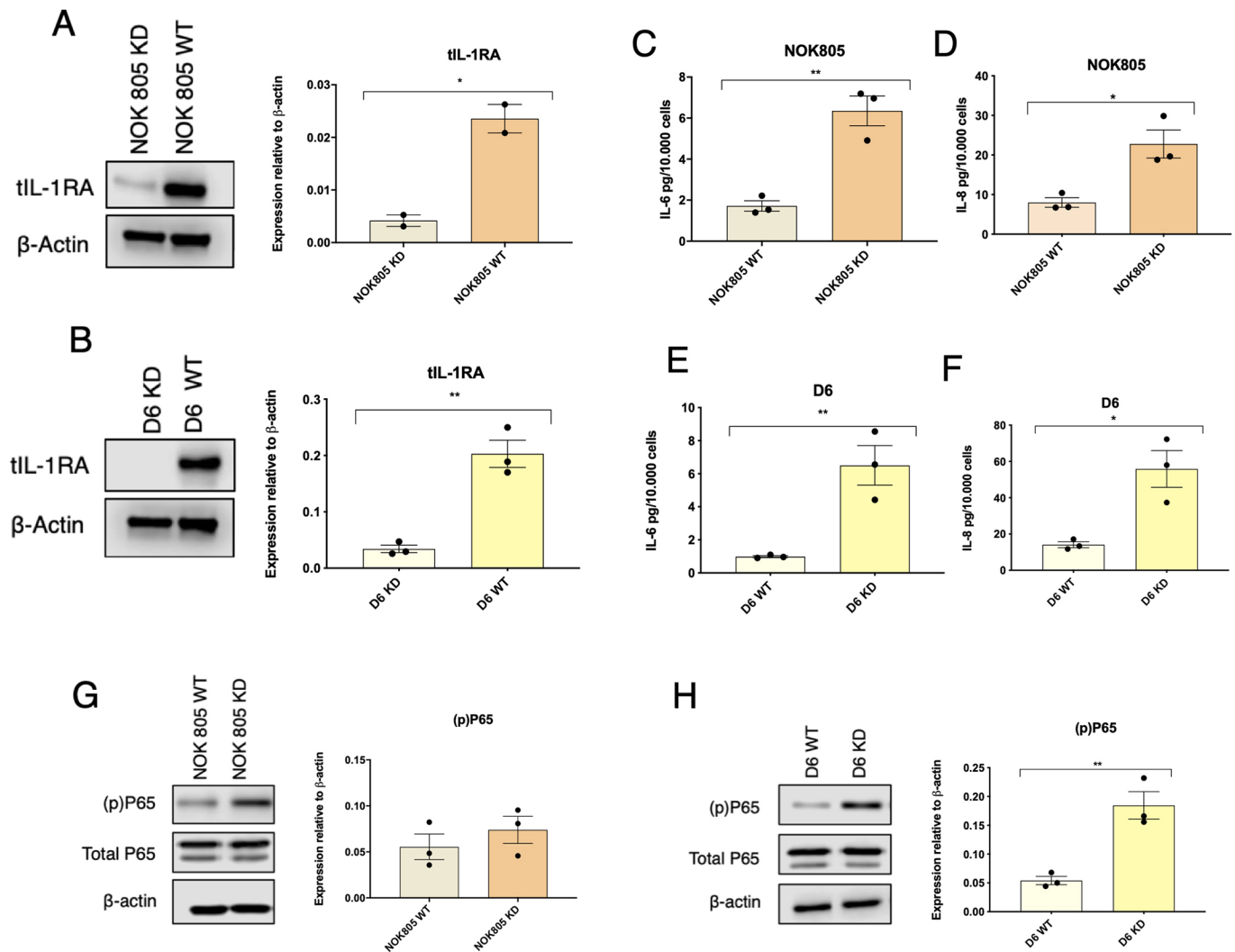
Fig. 3. icIL-1RA1 regulates IL-6 and IL-8 secretion in normal and dysplastic mortal oral keratinocytes. (A,B) icIL-1RA1 knock down in primary NOKs (A) and primary OD (B) after CRISPR/Cas9 gene editing. Quantification of tIL-1RA expression is represented as mean±s.e.m. (N=3 independent experiments). (C-F) IL-6 and IL-8 secretion by NOK805 cells (C,D) and D6 cells (E,F) after icIL-1RA1 gene editing (N=3 independent experiments, n=3 technical replicates). (G,H) Immunoblotting of p65 phosphorylation after icIL-1RA1 gene editing in NOK805 (G) and D6 (H) cells. Data are mean±s.e.m. (N=3 independent experiments). *P<0.05; **P<0.005 (unpaired two-tailed t-test).

keratinocytes, icIL-1RA1 might be involved in both the onset of senescence and in the development of the SASP, which are parallel but separate processes.

DISCUSSION

IL-1RA expression has been shown to decrease in OSCCs (Shiiba et al., 2015). Evidence from other cancers suggest that exogenous IL-1RA might be effective for the treatment of IL-1-expressing tumours, such as melanoma, gastric and breast cancers, among others (Dinarello, 2010). A recent paper showed that exogenous IL-1RA can interrupt the oral carcinogenesis process *in vivo*, as submucosal injections of IL-1RA into the tongue of mice during 4NQO-induced oral carcinogenesis interrupted the malignant transformation process (Wu et al., 2016). Nevertheless, the timing, role and consequences of IL-1RA loss of expression during the malignant transformation of oral keratinocytes have not been explored in detail.

We found icIL-1RA was progressively downregulated in oral dysplastic (in both mortal and immortal, but more profoundly in

immortal dysplasias) and oral carcinomatous cell lines, both at the mRNA and protein levels, but the mechanisms underlying the downregulation are not known. Post-transcriptional modifications such as methylation could be responsible for *IL1RN* downregulation in ODs and OSCCs, but only a small increase in methylation events of the IL-1RA promoter is evident in HNC (http://maplab.imppc. org/wanderer/), thus it is unlikely that this is the cause of loss of expression. *IL1RN* polymorphisms have been attributed to an increased risk of developing some cancers, like cervical gastric carcinomas (Wu et al., 2014; Zhang et al., 2012). Nevertheless, it is unlikely that this is the cause of loss of IL1-RN expression in OD and OSCC, as polymorphic genes are usually active and produce an abnormal form of the protein, which would not explain the decrease in *IL1RN* transcript levels and lack of protein expression in OD and OSCC cell lines. However, the mechanisms underlying *IL1RN* downregulation remain unclear. Other studies have also shown IL-1RA downregulation at mRNA and protein levels in OSCC (von Biberstein et al., 1996; Shiiba et al., 2015; Hakelius et al., 2016). There has been little focus on when *IL-1RN* downregulation
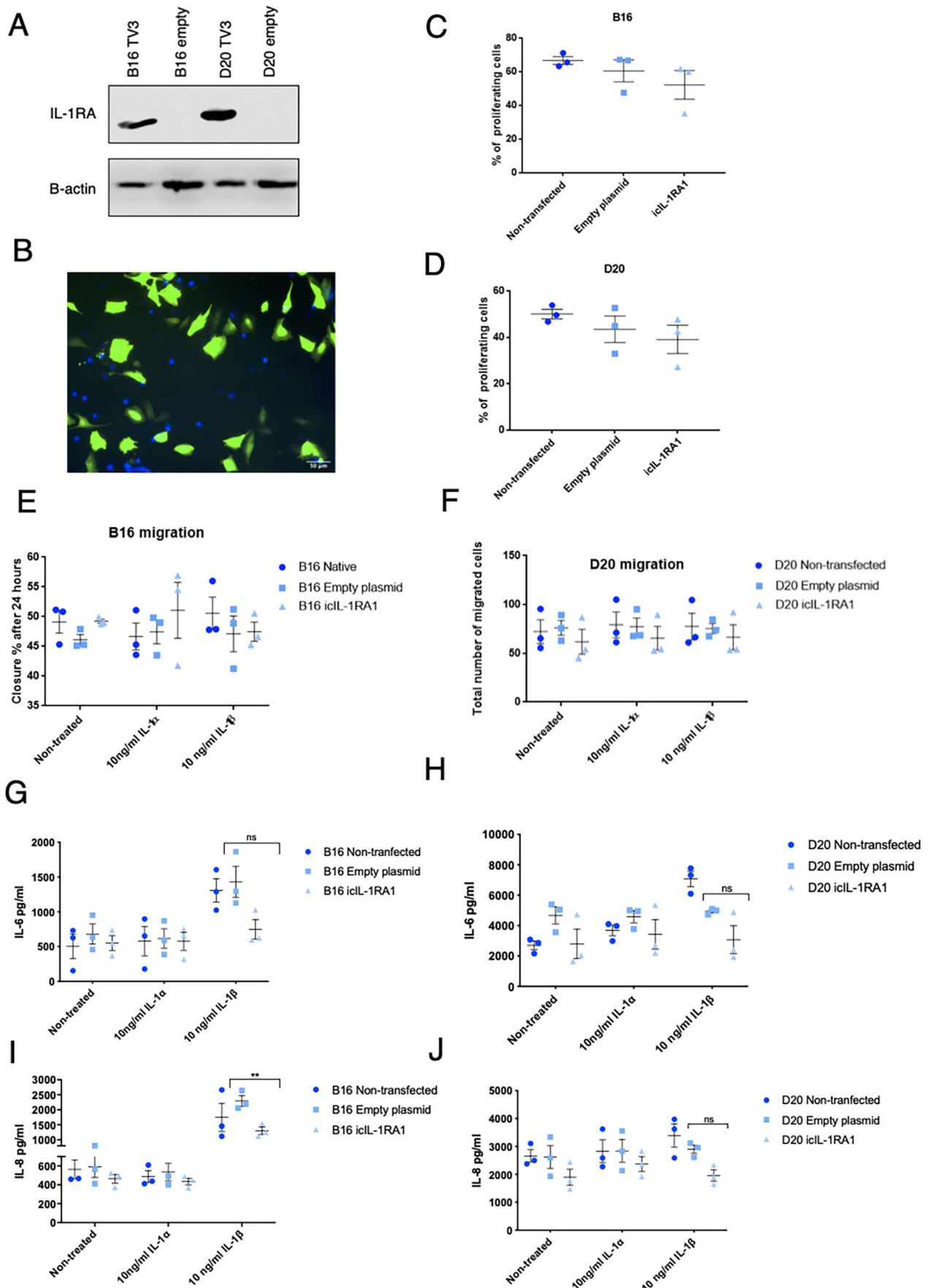
Fig. 4. See next page for legend.

Fig. 4. icIL-1RA1 does not modify proliferation or migration of OD and OSCC cells. (A,B) B16 and D20 cells were transfected with a pCMV6-Entry vector coding for icIL-1RA1 (A) with a transfection efficiency >50% (B). Blue, nuclei stained with DAPI; green cells, positive transfected cells with a vector encoding for GFP. Scale bar: 50 µm. (C,D) Proliferation was assessed using a Click-iT Plus EdU Flow Cytometry Assay in icIL-RA1 transfected, mock transfected and non-transfected B16 (C) and D20 (D) cells. (E) An ORIS migration assay was used to assess B16 migration after transfection with a pCMV6-Entry vector coding for icIL-1RA1, an empty plasmid and non-transfected. The migration of each group was assessed with no treatment, after treatment with 10 ng/ml of rIL-1α and 10 ng/ml of rIL-1β. (F) The migration of D20 cells after transfection was performed using the transwell system. The migration of each group (non-transfected, mock transfected and icIL-1RA1 transfected) was assessed with no treatment, after treatment with 10 ng/ml of rIL-1α and 10 ng/ml of rIL-1β. (G-J) IL-6 (G,H) and IL-8 (I,J) secretion after transfection with a pCMV6-Entry vector coding for icIL-1RA1, an empty plasmid and non-transfected. Secretion of both cytokines was assessed with no treatment, after treatment with 10 ng/ml of rIL-1α and 10 ng/ml of rIL-1β. Data are shown as mean±s.e.m. (N=3 independent experiments, and n=3 technical repeats). Statistical analysis was performed using one-way ANOVA (C,D) and two-way ANOVA (E-J). **$P<0.005$; ns, not significant.

happens in the oral carcinogenesis process. As shown by our results, reduced expression of IL-1RA in dysplastic cells suggests that IL-1RA downregulation can occur in early (precancer) stages of the carcinogenesis process. This has also been reported by Shiiba et al. (2015), who found IL-1RA protein expression to be progressively downregulated through OD to OSCC. Despite expression levels of sIL-1RN seeming to decrease in OD and OSCC cell lines compared to NOKs, there were no statistically significant differences between the groups. This is explained by the fact that the OD group is composed of a mixture of both immortal and mortal cell lines, and it is worth noting that sIL-1RN mRNA expression did decrease in immortal cells compared to mortal cells. No immortal NOKs were included in the NOK group, which meant that, overall, no statistically significant result was obtained.

There has been much discussion about the specific functions of icIL-1RA, and it has been hypothesized that its main function might be to counteract intracellular actions of IL-1α (Palmer et al., 2005). We found that IL-1RA was localized both in the cytoplasm and inside the nucleus of NOKs, which has also been reported in endothelial cells (Merhi-Soussi et al., 2005). Despite being immortal, the FNB6 cell line (immortalized NOKs) retained IL-1RA expression, possibly because it was immortalized at low passage number, where IL-1RA is high. Diffuse expression of IL-1RA in the cytoplasm of oral cells has been reported recently (Abé et al., 2017), but to our knowledge, we are the first group to report intranuclear IL-1RA expression in oral keratinocytes. This corresponds to our other finding that IL-1R1 also localizes both on the cell surface and inside or on the nucleus membrane of OD and OSCC cells. This is a novel finding, suggesting that intranuclear IL-1α (which is reported to act in a non-IL-1R1-dependent way) (Werman et al., 2004; Cheng et al., 2008) could also act in an IL-1R1-dependent manner, although that remains to be demonstrated. A recent report showed that full length IL-1α, which includes the nuclear localization sequence, is able to induce IL-1β, IL-6 and IL-8 secretion (Lau et al., 2019). IL-1R1 upregulation in immortal dysplastic and cancerous keratinocytes further highlights the deregulation of the whole IL-1 system during oral cancer development, re-enforcing our hypothesis that IL-1RA downregulation is important for the acquisition of a malignant phenotype.

Contrary to previous reports from skin and bladder cancer cell lines (La et al., 2001; Merhi-Soussi et al., 2005), we did not find any

effects of ectopic expression of icIL-1RA1 on migration or cell proliferation. It is likely that the main advantage of icIL-1RA1 downregulation in oral epithelial cells is to allow an increase in IL-6 and IL-8 production, probably by enabling increased NF-κB activation, as observed when icIL-1RA1 was knocked down in mortal NOK and OD cell cultures. Although this needs further validation, as these are observations from correlative data. Both IL-6 and IL-8 are considered as 'oncogenic cytokines', as they are able to cause epithelial-to-mesenchymal transition (Coppé et al., 2008), stimulate angiogenesis and tumour growth (Sparmann and Bar-Sagi, 2004; Ancrile et al., 2007), disrupt cell-cell communication, impede macrophage function and promote epithelial and endothelial cell migration and invasion (Loaiza and Demaria, 2016). The activation of NF-κB in head and neck squamous cell carcinoma (HNSCC) has been reported to have an important role in the malignant phenotype of HNSCC, as inhibiting NF-κB inhibited growth, survival and expression of IL-1α, IL-6, IL-8 and GM-CSF in a mouse HNC model (Duffey et al., 1999). In fibroblasts, the expression of IL-6 and IL-8 depends on NF-κB activation by the IL-1α/IL-1R1 axis, as IL-1α depletion has been shown to significantly reduce IL-6 and IL-8 levels by reducing DNA-binding activity of NF-κB in an IL-1R1-dependent manner (Orjalo et al., 2009). Interestingly, only treatment with recombinant IL-1β, and not recombinant IL-1α, had an effect on IL-6 and IL-8 production by the D20 and B16 oral dysplastic and oral cancer cell lines. A possible explanation for this is that those cell lines already exhibited high levels of endogenous IL-1α, thus adding more IL-1α had no effect, whereas IL-1β expression by oral cancer cell lines has been reported to be very low or undetectable (Al-Sahaf et al., 2019).

As IL-1 is important for the development of the SASP (Lau et al., 2019), and there is evidence linking the SASP with malignant transformation of pre-cancerous cells (Malaquin et al., 2013; Coppé et al., 2008; Ortiz-Montero et al., 2017; Lau et al., 2019), we decided to study the role of icIL-1RA during senescence of normal and dysplastic oral keratinocytes. icIL-1RA1 depletion in D6 cells increased the secreted levels of IL-6 and IL-8 in pre-senescent cells, and triggered premature senescence. In agreement with this, Uekawa et al. (2004) showed that depletion of IL-1RA in mouse embryonic fibroblasts triggered premature senescence, probably via activation of the p38 MAPK by IL-1β. Also, IL-1β has been reported to induce senescence in NOKs (Jang et al., 2015), and IL-1α has been shown to regulate the induction of senescence in a paracrine manner (Acosta et al., 2013). This suggests that icIL-1RA is an indirect regulator of the onset of senescence, by regulating IL-1 activity, which is important for the induction of senescence (Fig. 8). Nevertheless, according to a recent paper from Lau et al. (2019), both IL-1α and IL-1β are crucial for the development of the SASP in an IL-1R1-dependent manner, but are not essential for the triggering of senescence, as cells in which IL-1α and IL-1β have been inactivated still senesce (Lau et al., 2019).

We made the observation that CCFs were present in both normal and dysplastic senescent oral keratinocytes. This was correlated with a significant decrease in Lamin B1 expression, which suggested an increase in nuclear membrane permeability. CCF can initiate senescence by triggering the innate immunity cytosolic DNA-sensing cGAS-STING pathway (Dou et al., 2017). We inhibited cGAS in senescent ODs (D6 cell culture) with a cGAS inhibitor, RU.521 (Vincent et al., 2017). RU.521 significantly decreased secreted IL-6 levels when used at concentrations of 10 µg/ml and 20 µg/ml, with no changes observed in the secretion of IL-8 and IL-1β. Similar to these results, cGAS has been reported to regulate the SASP by decreasing IL-6 levels in vitro and in vivo
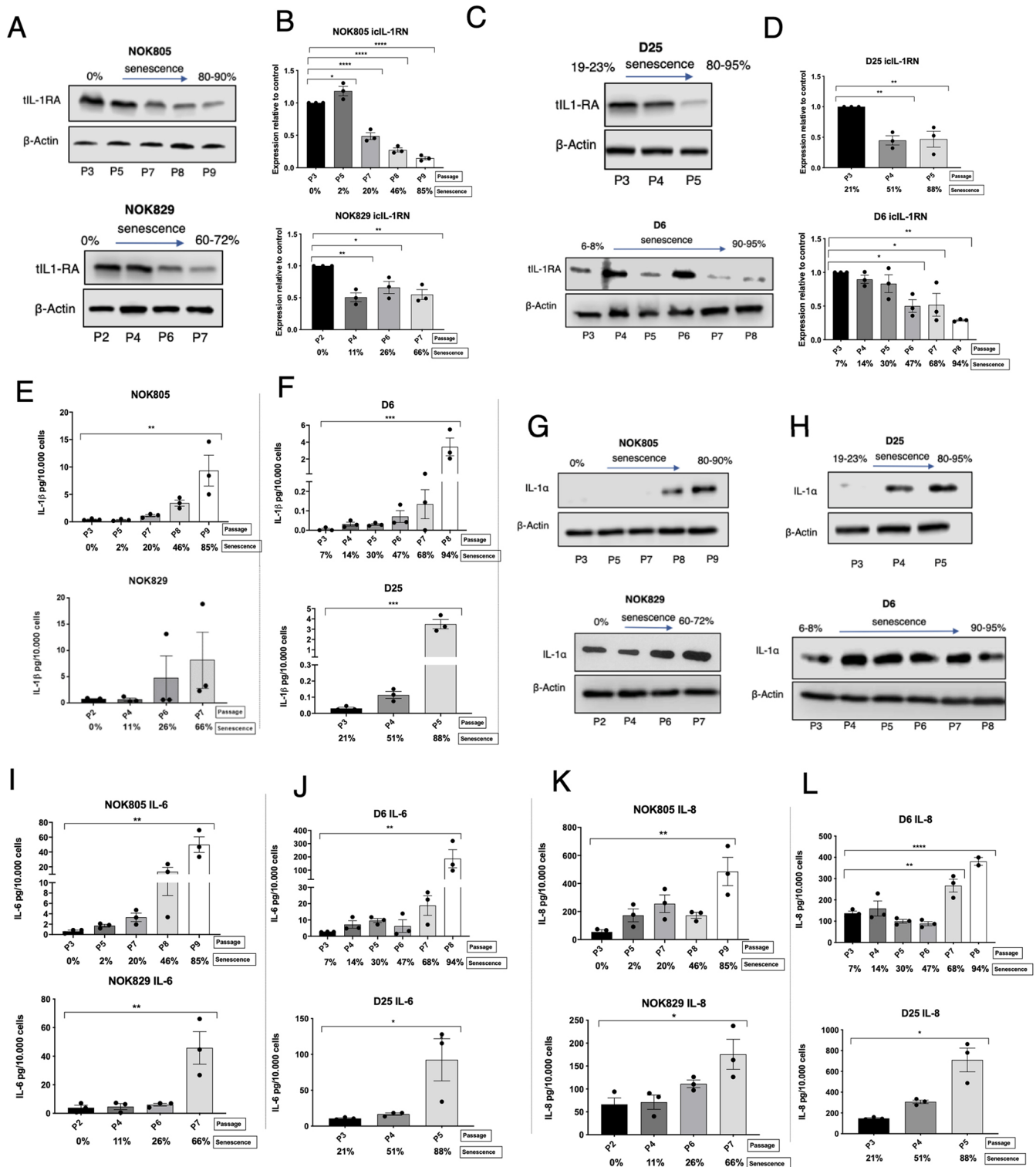
Fig. 5. icIL-1RA expression decreases, whereas IL-6, IL-8, IL-1α and IL-1β levels increase during replicative senescence. (A-D) Total IL-1RA protein expression and icIL-1RN transcript levels during replicative senescence of normal (A,B) and dysplastic (C,D) oral keratinocytes. (E,F) IL-1β secretion during replicative senescence of normal (E) and dysplastic (F) oral keratinocytes. (G,H) Immunoblotting showing IL-1α expression in normal (G) and dysplastic (H) oral keratinocytes during replicative senescence. (I-L) IL-6 and IL-8 secretion during replicative senescence of normal (I and K, respectively) and dysplastic (J and L, respectively) oral keratinocytes. Data are mean±s.e.m. (N=3 independent experiments, and n=2 technical repeats). Senescence percentage is based on the percentage of cells stained positive for SA-β-GAL. *P<0.05; **P<0.005; ***P≤0.0005; ****P≤0.00001 (one-way ANOVA).

(Glück et al., 2017). Interestingly, we observed a dose-dependent decrease in phosphorylated p65 and IL-1RA proteins levels, indicating a decrease in NF-κB activity. There was no evidence

that the effects of RU.521 arose as a consequence of cytotoxicity, as cell viability did not change between untreated and treated groups. These results indicate that the cGAS–STING pathway is activated
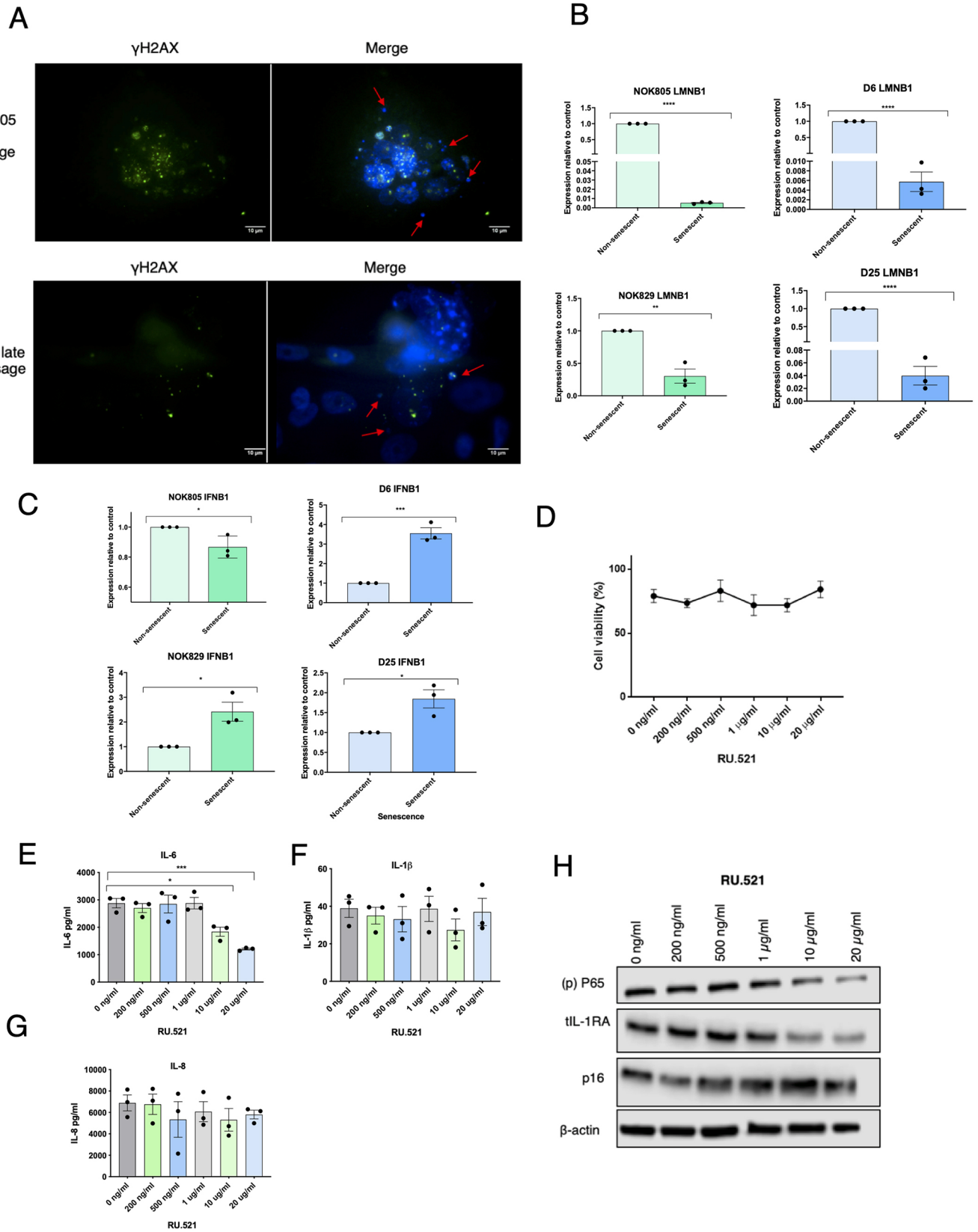
Fig. 6. See next page for legend.

during replicative senescence of oral keratinocytes, which has not been reported before. It also suggests that there is feedback regulation between the NF-κB pathway and IL-1RA, as knockout of IL-1RA resulted in an increase in p65 phosphorylation, whereas a decrease in p65 phosphorylation (by cGAS inhibition) resulted in a decrease in IL-1RA.

Fig. 6. cGAS is activated during replicative senescence of oral keratinocytes. (A) Immunofluorescence showing the presence of CCF in senescent NOK805 and D25 cells. Scale bars: 10 µm. (B) Lamin B1 (LMNB1) transcript levels in senescent normal (NOK805 and NOK829) and dysplastic (D6 and D25) oral keratinocytes (N=3 independent experiments, and n=3 technical repeats). (C) IFNB1 transcript levels in senescent normal and dysplastic oral keratinocytes (N=3 independent experiments). (D) Cell viability of D6 cells after treatment with different doses of RU.521 (N=3 independent experiments). (E-G) IL-6 (E), IL-1β (F) and IL-8 (G) secretion by D6 cells after treatment with RU.521 (N=3 independent experiments, and n=2 technical repeats). (H) Immunoblotting showing phosphorylation of P65, tIL-1RA and p16^{Ink4a} expression after treatment with RU.521. Data are mean±s.e.m. Statistical analysis was performed using an unpaired two-tailed t-test (B,C) and one-way ANOVA (E-G) (*P<0.05; ***P<0.0005; ****P<0.00001).

Altogether, our data suggests that icIL-1RA1 downregulation can potentially contribute to oral cancer development in two ways; by facilitating a pro-inflammatory state in non-senescent cells, and by allowing a premature and deregulated SASP, which are likely to be acting in combination (Fig. 8). icIL-1RA1 expression is lost early in the oral carcinogenesis process, often at the dysplasia stage, and is particularly seen when dysplastic cells achieve replicative immortality. This facilitates an increase in the activation of the NF-κB pathway, which supports the development of a pro-inflammatory state, with high levels of IL-6 and IL-8. If dysplastic cells (in which icIL-1RA1 expression is lost or decreased) are not removed over time, an inflammatory microenvironment will be generated. *In vivo*, it is very common to observe inflammatory infiltrate below the areas of epithelial dysplasia (Napier and Speight, 2008). Nevertheless, icIL-1RA1 downregulation results in an increase in IL-6 and IL-8, both of which can promote epithelial-to-mesenchymal transition (Coppé et al., 2008), and IL-6 can act as a mitogen in a paracrine fashion (Kuilman et al., 2008). In addition, inflammation has been shown to contribute to OSCC invasion (Goertzen et al., 2018). Thus, if the dysplastic cells with low levels of icIL-1RA1 are not eliminated, or the inflammatory response is not regulated, the imbalance in the inflammatory response could promote the development of an OSCC. In addition, ODs are a mixture of mortal and immortal cells (McGregor et al., 2002). Many mortal dysplastic cells will senesce as part of the DNA damage response, and normal keratinocytes will senesce as a consequence of replicative ageing. This will lead to the development of the SASP (which is overexpressed in OD compared to NOKs). This should be beneficial as it could prevent dysplastic cells from progressing into cancer. But not all dysplastic cells will senesce. Some will escape senescence, e.g. because of p16^{Ink4a} mutation or methylation, mutations or inactivation of p53 and reactivation of telomerase, and will become immortal (McGregor et al., 2002, 1997). Thus, the 'initiated' immortal cells are primed for malignant transformation, on which the SASP can act as a 'promoter' (Coppé et al., 2008; Ortiz-Montero et al., 2017). Supporting this idea is the fact that *in vivo*, all leukoplakias have some degree of p16^{Ink4a} expression, which is not related to HPV infection (Tomo et al., 2020), and the presence of γH2AX foci in OD is related to the risk of malignant transformation, and although γH2AX is a marker of genomic damage/instability, it does also mark senescent cells (Leung et al., 2017). Our findings suggest that targeting the IL-1 pathway by restabilising IL-1RA levels in ODs could be a useful approach to reduce malignant transformation of OPMDs.

MATERIALS AND METHODS
Cell culture
The isolation of primary NOKs was performed in accordance with The University of Sheffield Ethics Committee (approval reference 3463). The following cell lines/cell cultures used in this study have been described previously:

FNB6, D6, D25, B16, B22, D19, D20 (McGregor et al., 1997, 2002), OKF4 (Rheinwald et al., 2002) and OKF6 (Natarajan et al., 2006).

FNB6, OKF4, OKF6, B16, B22, D19, D20 cell lines were cultured in Dulbecco's modified Eagle medium (DMEM) low glucose (Sigma-Aldrich), containing 10% v/v fetal bovine serum (FBS) and 21% v/v F12 nutrient mix (Sigma-Aldrich), supplemented with 2 mM L-glutamine (Sigma-Aldrich), 6.25 µg/ml adenine, 100 µg/ml penicillin and 100 U/ml streptomycin (Sigma-Aldrich), 8.47 ng/ml cholera toxin, 10 ng/ml epidermal growth factor (EGF) (Sigma-Aldrich) and 5 µg/ml human insulin (Sigma-Aldrich). D6, D25, NOK805 and NOK829 cell cultures were grown using lethally irradiated (i) 3T3 feeders, as described previously (Rheinwald and Green, 1975), in DMEM low glucose (Sigma-Aldrich) containing 10% v/v fetal bovine serum (Hyclone FetalClone II Serum, Fisher Scientific) and 21% v/v F12 nutrient mix (Sigma-Aldrich), supplemented with 2 mM L-glutamine (Sigma-Aldrich), 0.25 µg/ml adenine, 100 µg/ml penicillin and 100 U/ml streptomycin (Sigma-Aldrich), 10 ng/ml EGF (Sigma-Aldrich), 1 mg/ml human insulin (Sigma-Aldrich), 0.4 µg/ml hydrocortisone, 1.36 ng/ml and 5 µg/ml 3,3′,5-tri-iodothyronine/apo-transferrin and 0.7 mM Na pyruvate (Sigma-Aldrich). All cell cultures were incubated at 37°C with 5% CO_2, and checked daily. The medium was replaced every 2 to 3 days and cells were passaged when ∼80-90% of confluency was achieved. All cell cultures were routinely tested for mycoplasma infection.

Confirmation of identity – short tandem repeat profiling
DNA was extracted from each cell type using a Wizard Genomic DNA Purification Kit (Promega) and sent for short tandem repeat profiling (Core Genomic Facility, Medical School, The University of Sheffield). No match was found for any of the cells tested, which was expected as none of the cell lines used had been previously registered, but the results were comparable to previous analysis. The lack of match also shows that contamination with other cell lines was unlikely.

Transient transfection
Approximately $2×10^5$ cells per well were seeded in six-well plates in growth medium free of antibiotics, and were left at 37°C and 5% CO_2 for 24 h. The next day, cells were ∼70-80% confluent and were transfected using FuGENE HD transfection reagent (Promega) following the manufacturer's recommendations. Cells were either transfected with a pCMV6-Entry vector coding for icIL-1RA1 or a pCDNA3.1 empty vector (Origene), and incubated at 37°C and 5% CO_2 for 48 h. After 48 h, cells were ready for experimentation and/or analysis. After every transfection procedure, immunoblotting was performed using an anti-IL-1RA antibody to confirm the presence of the transfected protein.

icIL-1RA1 KD
Intracellular IL-1RA1 KD was performed using the CRISPR/Cas9 system. Two commercially available sgRNAs (1 and 2) targeting a different segment of 20 nucleotides of exon 3 of the icIL-1RA1 gene were bought already incorporated into a pSpCas9 BB-2A-GFP vector (PX458) from GeneScript. The sgRNA sequences were as follows: sgRNA1 forward, 5′-TCCTCAGATAGAAGGTCTTC-3′, reverse, 5′-GAAGACCTTCTATCT-GAGGA-3′; sgRNA2 forward, 5′-CTAGTTGCTGGATACTTGCA-3′, reverse, 5′-TGCAAGTATCCAGCAACTAG-3′. NOK805 and D6 cells were seeded into six-well plates at a density of $2.5×10^5$ cells per well in antibiotic free medium with 10 µg/ml Y-27632 (Abcam) and left to adhere at 37°C and 5% CO_2. Y-27632 (Abcam) was used to facilitate cell growth and to avoid the induction of senescence. After 24 h, cells were transfected using JetPrime (Polyplus) following the manufacturer's recommendations. Twenty-four hours after transfection, cells were resuspended in growth medium and sorted using a FACSAria IIu cell sorter (BD Biosciences). The machine was previously calibrated with non-transfected cells of each cell type and baseline for fluorescence was set. Cells were divided into GFP$^+$ and GFP$^−$ cells, and same number of cells were collected per group. The gate was adjusted strictly to diminish the chance of getting any false positives into the GFP$^+$ group. GFP$^−$ cells were used as controls for all downstream assays. Single colony expansion could not be performed as both cell types used (NOK805 and D6 cell cultures) did not grow in isolation. GFP$^−$ and
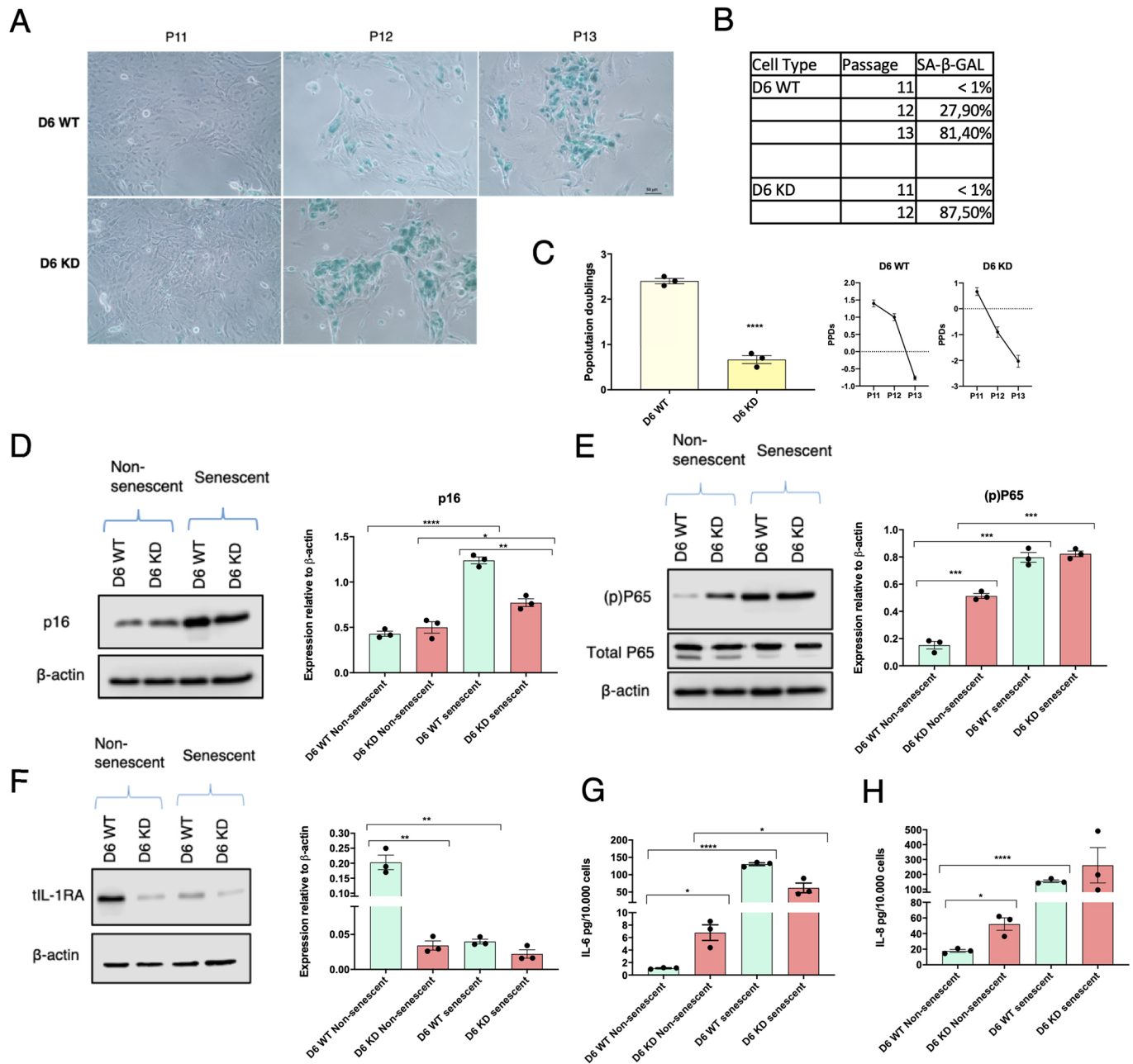
Fig. 7. icIL1.RA1 regulates the onset of senescence and the SASP. (A,B) SA-β-GAL activity after cell passaging in WT and icIL-1RA1 KD D6 cells. Scale bar: 50 µm. (C) Comparison of population doublings between WT and icIL-1RA1 KD D6 cells, and population doublings of each cell type at every passage (*N*=3 independent experiments and *n*=3 technical repeats). (D-F) Immunoblotting showing p16^{Ink4a} (D), phosphorylation of p65 (E) and tIL-1RA levels in non-senescent and senescent WT and icIL-1RA1 KD D6 cells (F) (*N*=3 independent experiments). (G,H) IL-6 and IL-8 secretion using the same samples from D-F (*N*=3 independent experiments, *n*=2 technical repeats). Data are mean±s.e.m. Statistical analysis was performed using an unpaired two-tailed *t*-test (C) or one-way ANOVA (D-H) (**P*<0.05; ***P*<0.005; ****P*<0.0005; *****P*<0.00001).

GFP$^+$ cells were grown under the same conditions and analysed or used at the same passage number.

Genomic DNA (gDNA) was extracted from each of the GFP$^+$ and GFP$^-$ cell types using a Wizard Genomic DNA Purification Kit and quantified using a Nanodrop 1000 Spectrophotometer (Thermo Fisher Scientific). Primers targeting a sequence surrounding and including both sgRNA target sites were designed (forward, 5′-GCTGGGCACATGGTGGCTGT-3′; reverse, 5′-ATGCCCACATACATTGGCTT-3′), and PCR reactions for each of the gDNAs were performed as follows: 5 min at 95°C and 30 cycles of 95°C for 60 s, 55°C for 60 s and 72°C for 30 s, followed by 2 min at 72°C. PCR products were run in a 2% agarose gel for 90 min at 90 V and visualized using the InGenius3 gel documentation system (Syngene). PCR

bands were extracted from the agarose gel and purified using an Isolate II PCR and gel kit (Bioline), and sent for Sanger sequencing (GATC Biotech, Eurofins Genomics). Sequences obtained from WT cells were aligned with the expected sequence to corroborate proper primer amplification. This was carried out using the multiple sequence alignment tool of the European Bioinformatics Institute (EMBL-EBI) (www.ebi.ac.uk/Tools/msa/clustalo/). In order to confirm a successful editing event, the sequences obtained from WT and CRISPR-edited cells were aligned.

Senescence assays

NOKs (NOK805 and NOK829 cell cultures) and mortal ODs (D6 and D25 cell cultures) were grown in combination with i3T3 in T25 cm^2 tissue culture
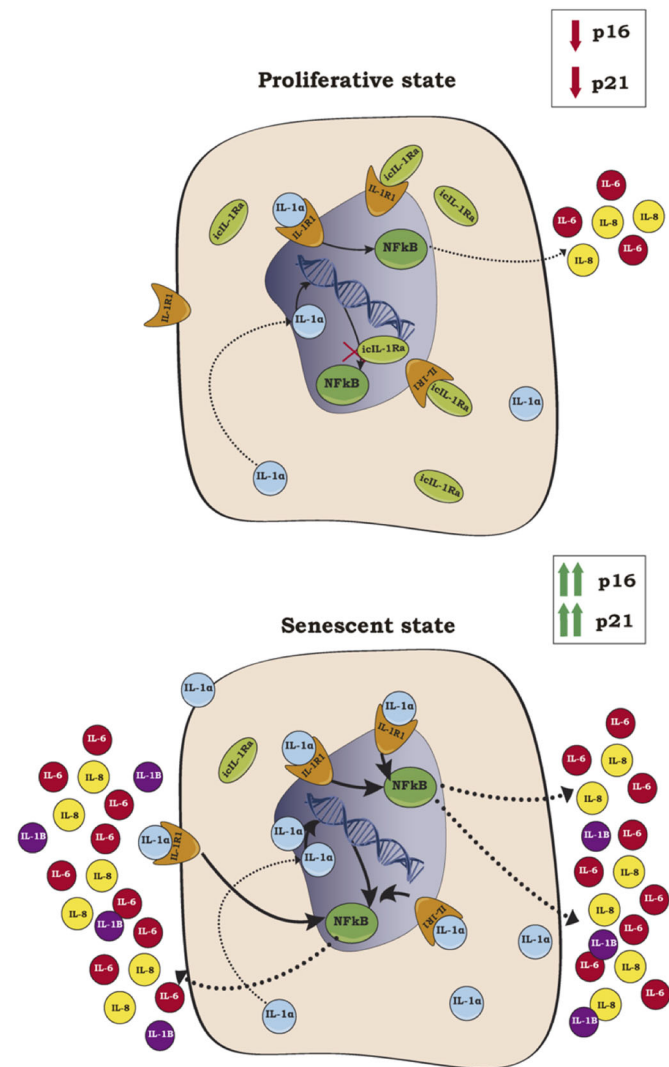
Fig. 8. A proposal of how icIL-1RA1 might regulate senescence and the SASP in oral keratinocytes. If icIL-1Ra1 expression decreases, IL-1α can bind to more IL-1R1 receptor, and intranuclear IL-1α can interact with the nucleus with no or less regulation, which would increase the activation of the NF-κB pathway. This will lead to the production of more IL-1α and IL-1β (IL-1β is not constitutively produced by oral keratinocytes), and to high levels of IL-6 and IL-8, which will induce and re-enforce the senescent state.

flasks until replicative senescence was achieved. Cells were passaged when they achieved a confluency of 70-85%. Before trypsinization, conditioned medium was stored at −20°C and i3T3 feeders were removed by incubating them with 0.02% EDTA solution for 3 to 5 min at 37°C and 5% CO$_2$. After every passage, senescence-associated β-galactosidase activity was quantified.

Senescence associated β-galactosidase staining
Twenty thousand cells per well were seeded in a 12-well plate and left to adhere overnight. Senescence associated β-galactosidase activity was assessed using a senescence detection kit (ab65351, Abcam) following the manufacturer's recommendations.

Proliferation assay
Proliferation was assessed with the Click-iT Plus EdU Flow Cytometry Assay (Invitrogen) following the manufacturer's recommendations.

Migration assays
To assess migration properly, cell proliferation was inhibited with mitomycin C. Mitomycin C concentration was optimised using plots of cell replication

(CellTrace, Invitrogen) through flow cytometry. Concentrations of 0.5 μg/ml and 2 μg/ml were used to inhibit cell growth of B16 and D20 cell lines, respectively.

For the B16 cell line, migration was assessed using the ORIS cell migration assay (Platypus Technologies) following the manufacturer's recommendations. For the D20 cell lines, the transwell migration assay was used, as those cells were not suitable for the ORIS cell migration assay. Before seeding the cells, the external surface of the membrane (PET membrane, 8.0 μm, 24-well inserts, Falcon) was coated with fibronectin. This was achieved by adding 100 μl of 10 μg/ml fibronectin (Sigma-Aldrich) and incubating each insert for 1 h at 37°C. After this time, 100 μl and 300 μl of 1% bovine serum albumin (BSA) serum-free medium was added inside the insert and on the bottom well, correspondingly. Each plate was incubated for 1 h at 37°C. This was carried out to block non-specific binding. Once the inserts were properly coated with fibronectin, cells were trypsinized, centrifuged at 200 g for 5 min and re-suspended in 1% BSA serum-free medium. The cell suspension was further diluted in order to achieve the desired cell concentration. In-between, 500 μl of 10% FBS containing medium and mitomycin C at a concentration of 2 μg/ml were added. Once this was completed, 100 μl of cell suspension containing ∼25,000 cells was added into each insert and incubated for 3.5 h at 37°C and 5% CO$_2$. After this, the medium from each bottom well was removed (in order to remove the mitomycin C) and 500 μl of 10% FBS containing medium with rIL-1α (10 ng/ml), rIL-1β (10 ng/ml) or nothing extra was added to each bottom well and incubated for 24 h at 37°C and 5% CO$_2$. The next day, medium was removed, each insert was washed once in PBS and fixed for at least 20 min in 10% formalin. The inserts were then washed once in distilled water and stained for 30 min in a solution of 0.5% (w/v) Crystal Violet in 10% ethanol. Following this, the inserts were washed 2-3 times in distilled water before proceeding to the mounting stage. The cells attached to the inner part of the membrane (top), were swabbed away using a cotton bud in order to keep only the cells that migrated from the inner side (top) to the outer side (bottom) of the membrane. The membranes were then removed from the insert by cutting them carefully with a scalpel blade, and were then mounted on glass slides using DPX mounting medium (Merck). Three pictures of each experimental membrane were taken using an Olympus BX51 optical microscope at 20× magnification, and cells were counted using Fiji ImageJ.

cGAS inhibition assay
Mortal dysplastic keratinocytes (D6) were grown until replicative senescence was achieved (evaluated by SA-β-Gal activity). A total of 160×10^4 senescent cells were seeded in 12-well plates and left overnight to adhere. D6 senescent cells were then treated for 24 h with different concentrations of the cGAS inhibitor RU.521 (0 ng/ml, 200 ng/ml, 500 ng/ml, 1 μg/ml, 10 μg/ml and 20 μg/ml) (InvivoGen). After 24 h incubation at 37°C and 5% CO$_2$, conditioned medium was collected and cells were harvested for analysis. Each individual repeat was counted, and the proportion of live/dead cells was calculated for each experimental group. This was carried out by staining the cells with Trypan Blue (Thermo Fisher Scientific) and counting them using a haemocytometer.

Immunofluorescence
Between 20,000 and 40,000 cells were seeded in eight-well tissue culture chambers (Starstedt) and incubated for 24 h at 37°C and 5% CO$_2$. Cells were then washed three times with PBS and fixed with 4% paraformaldehyde (Santa Cruz Biotechnology) for 10 min. After fixation, cells were washed three times with PBS and blocked for 1 h with 0.2% Triton X-100 and 3% BSA (Sigma-Aldrich) in PBS. After blocking, the cells were washed three times with PBS and incubated with primary antibody at working concentration in 3% BSA for 1 to 2 h. The primary antibodies used were as follows: goat anti-IL-1RA IgG (1:500, AF-280-NA, R&D Systems) and mouse anti-γH2AX IgG (1:200, JBW301, Merck Millipore). Negative controls were incubated without the primary antibody under the same conditions. Samples were then washed three times with PBS and incubated with conjugated secondary antibody in 3% BSA for 1 h under darkness. The secondary antibodies used were as follows: Alexa Fluor 594 donkey anti-goat IgG (1:1000, A11058, Thermo Fisher Scientific) and Alexa Fluor 488

goat anti-mouse IgG (1:1000, A11001, Thermo Fisher Scientific). After secondary antibody incubation, the samples were washed three times with PBS followed by three washes with distilled H_2O, and were mounted using Prolong Gold antifade mountant with DAPI (Invitrogen). The slides were left to set for 24 h in the dark at 4°C before visualization. Samples were visualized using a Zeiss 880 AiryScan confocal microscope or a Zeiss Axioplan 2 Fluorescent microscope. Images were then processed using Fiji ImageJ. Negative controls of each individual cell line were processed together with each sample using the same settings.

For double labelling, cells were blocked in a solution of 10% goat serum (the species in which the first secondary antibody was raised) with 0.2% Triton X-100 in PBS. The samples were then incubated with the first primary antibody (an anti-IL-1R1 antibody, 1:100, MAB269, R&D Systems). Negative controls were incubated in the same solution without the primary antibody. The secondary antibody used was a goat anti-mouse Alexa Fluor 594 IgG (Thermo Fisher Scientific), at a concentration of 1:1000. After incubation with the first secondary antibody for 1 h, the samples were washed three times with PBS and then blocked with a solution of 10% rat serum with 0.2% Triton X-100 in PBS for 60 min. After this, the cells were washed three times with PBS and were incubated with the second primary antibody, an anti β-actin antibody (A1978, Sigma-Aldrich), at a concentration of 1:200 in a solution of 3% BSA with 0.2% Triton X-100 in PBS for 1 h. Negative controls were incubated in the same solution without the primary antibody. After this, the samples were washed three times with PBS and incubated in the second secondary antibody, a goat anti-mouse Alexa Fluor 488 IgG (H+L) (1:1000, Thermo Fisher Scientific) in a solution of 3% BSA serum with 0.2% Triton X-100 in PBS for 1 h. The next steps were carried out as described above.

Immunohistochemistry
Immunohistochemistry for IL-1RA was performed on 4 μm formalin-fixed paraffin-embedded sections. Human skin sections were used as positive controls. Antigen retrieval was performed with heat-induced epitope retrieval in sodium citrate buffer (10 mM sodium citrate, 0.05% Tween 20, pH 6.0). The primary antibody used was goat IgG anti-IL-1RA (1:500, AF-280-NA, R&D Systems), and samples were incubated overnight at 4°C. After secondary antibody incubation, staining was visualized using a Vectastain ABC Kit (Vector Laboratories) with 3,3′-diaminobenzidine substrate and a haematoxylin counterstain. Staining was assessed in a semi-quantitative manner using a modified quickscore, accounting for both the extent and intensity of staining (Detre et al., 1995).

ELISA
Secreted IL-6, IL-8 and IL-1β were quantified using the BD OptEIA (BD Biosciences) sets for human IL-6, IL-8 and IL-1β detection. The procedure was performed following the manufacturer's recommendation using 96-well plates. Absorbance was read at 450 nm within 30 min of adding the stop solution. Wavelength correction was calculated by subtracting the absorbance at 570 nm from the absorbance at 450 nm.

qPCR
Total RNA was extracted from cell pellets using an Isolate II RNA Mini Kit (Bioline), following the manufacturer's instructions. RNA was quantified using a Nanodrop 1000 Spectrophotometer (Thermo Fisher Scientific). Five hundred nanograms of isolated RNA was reverse transcribed using a High Capacity cDNA Reverse Transcription Kit (Applied Biosystems), following the manufacturer's protocol using a Peltier thermal cycler (MJ Research). cDNA was then stored at −20°C.

Gene expression was quantified using a Rotor-gene Q real-time PCR cycler (Qiagen) with SYBR green or TaqMan chemistry. Quantification was achieved using delta CT values normalized to either U6 or B2M. Each reaction was performed in triplicate. All reactions were performed in total volumes of 10 μl, loading 500 ng of cDNA. The standard thermal cycle settings for a reaction consisted of 40 cycles, including a melt curve analysis (when using SYBR green). One cycle consisted of: 95°C for 10 s, 60°C for 15 s and 72°C for 20 s. SYBR green primers were designed in-house and bought from Sigma-Aldrich, corresponding to the following: icIL1RA, forward, 5′-CAGAAGACCTCCTGTCCTATGA-3′, reverse, 5′-

GAAGGTCTTCTGGTTAACATCCCAG-3′; sIL-1RA, forward, 5′-GAA-TGGAAATCTGCAGAGGCCTCCGC-3′, reverse, 5′-GAAGGTCTTCT-GGTTAACATCCCAG-3′; IL-1R2, forward, 5′-GTACGTGTTGGTA-ATGGGAGTTTC-3′, reverse, 5′-CCGCTTGTAATGCCTCCCACGAA-A-3′; IFN-β, forward, 5′-AAACTCATGAGCAGTCTGCA-3′, reverse, 5′-AGGAGATCTTCAGTTTCGGAGG-3′; Lamin B1, forward, 5′-CTCTC-GTCGCATGCTGACAG-3′, reverse, 5′-TCCCTTATTTCCGCCATCTCT-3′. TaqMan probes were bought from Thermo Fisher Scientific and corresponded to the following: IL1RN (Hs: 00277299), IL-1R1 (Hs: 00991010), IL-1α (Hs: 00174092), IL-6 (Hs: 00985639), IL-8 (Hs: 00174103), B2M (Hs: 4325797).

Western blotting
Protein was extracted by dissolving the cell pellets in an appropriate volume of lysis buffer on ice. The lysis buffer consisted of one tablet of complete mini-EDTA free protease inhibitor cocktail (Roche) and one tablet of phosphatase inhibitors (PhosSTOP, Roche) dissolved in 10 ml RIPA Buffer (Sigma-Aldrich). Cell suspensions were left for 30 min on ice and centrifuged at 19,700 g for 10 min at 4°C. The supernatants were stored at −20°C and the pellets were discarded. Protein quantification was performed using the bicinchoninic acid assay (Thermo Fisher Scientific), according to the manufacturer's protocol, using a TECAN spectrophotometer (Spark).

Ten to fifty micrograms of protein were mixed with 2× SDS lysis buffer, heated for 5 min at 95°C and then loaded into 12-15% SDS-PAGE gels. Gels were run for ~90 min at 150 V and transferred onto nitrocellulose or PVDF membranes using the Trans-Blot Turbo Transfer System (Bio-Rad) according to the manufacturer's instructions. After transfer, membranes were blocked with 5% milk (Marvel) in Tris-buffered saline (10 mM) containing 0.5% Tween 20 (v/v) (TBS-T) for 1 h at room temperature on a rocking platform. The membranes were then incubated for 1 h at room temperature or overnight at 4°C on a rocking platform with the primary antibody at a working concentration in 5% TBS-T milk. After incubation, membranes where washed three times for 10 min intervals with TBS-T and incubated with the secondary antibody at a working concentration in 5% TBS-T milk for 1 h at room temperature on a rocking platform. The membranes were then washed two times at intervals of 10 min with TBS-T and one time with TBS for 10 min, at which point they were ready for development. Membranes were developed with enhanced chemiluminescence (ECL), using Pierce ECL western blotting substrate (Thermo Fisher Scientific), according to the manufacturer's instructions. Signal was detected by exposure to an X-ray film (Thermo Fisher Scientific) in a dark room and developed using a Compact X4 Developer (Xograph Imaging Systems) or alternatively using a Li-Cor C-Digit Western Blot Scanner and Image Studio Software. Densitometry was performed using the Image Studio Software. Bands were manually selected using the drawing tool and the intensity of each band was normalized to the corresponding β-actin intensity.

Primary antibodies used were as follows: anti-IL-1RA (1:2000, AF-280-NA, R&D Systems); anti-p16[Ink4a] (1:1000, 108349, Abcam); anti-p21[Waf1/Cip1] (1:1000, MAB1047, R&D Systems); anti-phosphorylated p65 (1:1000, 3033, Cell Signaling Technology); and anti-IL-1α (1:1000, Ab134908, Abcam), anti-β-actin (1:10,000, A1978, Sigma-Aldrich). Secondary antibodies used were as follows: anti-mouse IgG horseradish peroxidase (HRP)-conjugated (1:5000, GTX221667-01, Genetex); anti-goat IgG HRP-conjugated (1:1000, HAF 017, R&D Systems); and anti-rabbit IgG HRP-conjugated (1:3000, 7074S, Cell Signaling Technology).

Statistical analysis
Statistical analysis was carried out using GraphPad Prism 7 Software. Comparison of two groups was performed using an unpaired Student's t-test. When the comparison included more than two groups, one-way ANOVA was performed. Two-way ANOVA was used when comparing two variables in multiple groups. $P < 0.05$ was considered statistically significant. The number of biological repeats is expressed as 'N=' and the number of technical repeats as 'n='.

References

Abé, T., Maruyama, S., Yamazaki, M., Xu, B., Babkair, H., Sumita, Y., Cheng, J., Yamamoto, T. and Saku, T. (2017). Proteomic and histopathological characterization of the interface between oral squamous cell carcinoma invasion fronts and non-cancerous epithelia. *Exp. Mol. Pathol.* **102**, 327-336. doi:10.1016/j.yexmp.2017.02.018

Acosta, J. C., Banito, A., Wuestefeld, T., Georgilis, A., Janich, P., Morton, J. P., Athineos, D., Kang, T.-W., Lasitschka, F., Andrulis, M. et al. (2013). A complex secretory program orchestrated by the inflammasome controls paracrine senescence. *Nat. Cell Biol.* **15**, 978-990. doi:10.1038/ncb2784

Al-Sahaf, S., Hunter, K. D., Bolt, R., Ottewell, P. D. and Murdoch, C. (2019). The IL-1/IL-1R axis induces greater fibroblast-derived chemokine release in human papillomavirus-negative compared to positive oropharyngeal cancer. *Int. J. Cancer* **144**, 334-344. doi:10.1002/ijc.31852

Alevizos, I., Mahadevappa, M., Zhang, X., Ohyama, H., Kohno, Y., Posner, M., Gallagher, G. T., Varvares, M., Cohen, D., Kim, D. et al. (2001). Oral cancer in vivo gene expression profiling assisted by laser capture microdissection and microarray analysis. *Oncogene* **20**, 6196-6204. doi:10.1038/sj.onc.1204685

Ancrile, B., Lim, K.-H. and Counter, C. M. (2007). Oncogenic Ras-induced secretion of IL6 is required for tumorigenesis. *Genes Dev.* **21**, 1714-1719. doi:10.1101/gad.1549407

Arend, W. R. (2002). The balance between IL-1 and IL-1Ra in disease. *Cytokine Growth Factor. Rev.* **13**, 323-340. doi:10.1016/S1359-6101(02)00020-5

Campisi, J. (2005). Senescent cells, tumor suppression, and organismal aging: good citizens, bad neighbors. *Cell* **120**, 513-522. doi:10.1016/j.cell.2005.02.003

Chapman, S., Mcdermott, D. H., Shen, K., Jang, M. K. and Mcbride, A. A. (2014). The effect of Rho kinase inhibition on long-term keratinocyte proliferation is rapid and conditional. *Stem Cell Res. Ther.* **5**, 60. doi:10.1186/scrt449

Cheng, W., Shivshankar, P., Zhong, Y., Chen, D., Li, Z. and Zhong, G. (2008). Intracellular interleukin-1α mediates interleukin-8 production induced by Chlamydia trachomatis infection via a mechanism independent of type I interleukin-1 receptor. *Infect. Immun.* **76**, 942-951. doi:10.1128/IAI.01313-07

Choi, P. and Chen, C. (2005). Genetic expression profiles and biologic pathway alterations in head and neck squamous cell carcinoma. *Cancer* **104**, 1113-1128. doi:10.1002/cncr.21293

Colotta, F., Dower, S. K., Sims, J. E. and Mantovani, A. (1994). The type II 'decoy' receptor: a novel regulatory pathway for interleukin 1. *Immunol Today* **15**, 562-566. doi:10.1016/0167-5699(94)90217-8

Coppé, J.-P., Patil, C. K., Rodier, F., Sun, Y., Muñoz, D. P., Goldstein, J., Nelson, P. S., Desprez, P.-Y. and Campisi, J. (2008). Senescence-associated secretory phenotypes reveal cell-nonautonomous functions of oncogenic RAS and the p53 tumor suppressor. *PLoS Biol.* **6**, e301. doi:10.1371/journal.pbio.0060301

Cromer, A., Carles, A., Millon, R., Ganguli, G., Chalmel, F., Lemaire, F., Young, J., Dembélé, D., Thibault, C., Muller, D. et al. (2004). Identification of genes associated with tumorigenesis and metastatic potential of hypopharyngeal cancer by microarray analysis. *Oncogene* **23**, 2484-2498. doi:10.1038/sj.onc.1207345

Davalos, A. R., Coppe, J.-P., Campisi, J. and Desprez, P.-Y. (2010). Senescent cells as a source of inflammatory factors for tumor progression. *Cancer Metastasis Rev.* **29**, 273-283. doi:10.1007/s10555-010-9220-9

Detre, S., SACLANI Jotti, G. and Dowsett, M. (1995). A "quickscore" method for immunohistochemical semiquantitation: validation for oestrogen receptor in breast carcinoma. *J. Clin. Pathol.* **48**, 876-878. doi:10.1136/jcp.48.9.876

Dinarello, C. A. (2010). Why not treat human cancer with interleukin-1 blockade? *Cancer Metastasis Rev.* **29**, 317-329. doi:10.1007/s10555-010-9229-0

Dou, Z., Ghosh, K., Vizioli, M. G., Zhu, J., Sen, P., Wangensteen, K. J., Simithy, J., Lan, Y., Lin, Y., Zhou, Z. et al. (2017). Cytoplasmic chromatin triggers inflammation in senescence and cancer. *Nature* **550**, 402-406. doi:10.1038/nature24050

Duffey, D. C., Chen, Z., Dong, G., Ondrey, F. G., Wolf, J. S., Brown, K., Siebenlist, U. and VAN Waes, C. (1999). Expression of a dominant-negative mutant inhibitor-kappaBalpha of nuclear factor-kappaB in human head and neck squamous cell carcinoma inhibits survival, proinflammatory cytokine expression, and tumor growth in vivo. *Cancer Res.* **59**, 3468-3474.

Eisenberg, S. P., Evans, R. J., Arend, W. P., Verderber, E., Brewer, M. T., Hannum, C. H. and Thompson, R. C. (1990). Primary structure and functional expression from complementary DNA of a human interleukin-1 receptor antagonist. *Nature* **343**, 341-346. doi:10.1038/343341a0

Garat, C. and Arend, W. P. (2003). Intracellular IL-1Ra type 1 inhibits IL-1-induced IL-6 and IL-8 production in Caco-2 intestinal epithelial cells through inhibition of p38 mitogen-activated protein kinase and NF-κB pathways. *Cytokine* **23**, 31-40. doi:10.1016/S1043-4666(03)00182-0

Glück, S., Guey, B., Gulen, M. F., Wolter, K., Kang, T.-W., Schmacke, N. A., Bridgeman, A., Rehwinkel, J., Zender, L. and Ablasser, A. (2017). Innate immune sensing of cytosolic chromatin fragments through cGAS promotes senescence. *Nat. Cell Biol.* **19**, 1061-1070. doi:10.1038/ncb3586

Goertzen, C., Mahdi, H., Laliberte, C., Meirson, T., Eymael, D., Gil-Henn, H. and Magalhaes, M. (2018). Oral inflammation promotes oral squamous cell carcinoma invasion. *Oncotarget* **9**, 29047-29063. doi:10.18632/oncotarget.25540

Guo, Y., Ayers, J. L., Carter, K. T., Wang, T., Maden, S. K., Edmond, D., Newcomb P., P., Li, C., Ulrich, C., Yu, M. et al. (2019). Senescence-associated tissue microenvironment promotes colon cancer formation through the secretory factor GDF15. *Aging Cell* **18**, e13013. doi:10.1111/acel.13013

Hakelius, M., Reyhani, V., Rubin, K., Gerdin, B. and Nowinski, D. (2016). Normal oral keratinocytes and head and neck squamous carcinoma cells induce an innate response of fibroblasts. *Anticancer Res.* **36**, 2131-2137.

Hannum, C. H., Wilcox, C. J., Arend, W. P., Joslin, F. G., Dripps, D. J., Heimdal, P. L., Armes, L. G., Sommer, A., Eisenberg, S. P. and Thompson, R. C. (1990). Interleukin-1 receptor antagonist activity of a human interleukin-1 inhibitor. *Nature* **343**, 336-340. doi:10.1038/343336a0

Haskill, S., Martin, G., van Le, L., Morris, J., Peace, A., Bigler, C. F., Jaffe, G. J., Hammerberg, C., Sporn, S. A., Fong, S. et al. (1991). cDNA cloning of an intracellular form of the human interleukin 1 receptor antagonist associated with epithelium. *Cell Biol.* **88**, 3681-3685. doi:10.1073/pnas.88.9.3681

Jang, D. H., Bhawal, U. K., Min, H.-K., Kang, H. K., Abiko, Y. and Min, B.-M. (2015). A transcriptional roadmap to the senescence and differentiation of human oral keratinocytes. *J. Gerontol. A Biol. Sci. Med. Sci.* **70**, 20-32. doi:10.1093/gerona/glt212

Koike, H., Uzawa, K., Nakashima, D., Shimada, K., Kato, Y., Higo, M., Kouzu, Y., Endo, Y., Kasamatsu, A. and Tanzawa, H. (2005). Identification of differentially expressed proteins in oral squamous cell carcinoma using a global proteomic approach. *Int. J. Oncol.* **27**, 59-67. doi:10.3892/ijo.27.1.59

Kuilman, T., Michaloglou, C., Vredeveld, L. C. W., Douma, S., van Doorn, R., Desmet, C. J., Aarden, L. A., Mooi, W. J. and Peeper, D. S. (2008). Oncogene-induced senescence relayed by an interleukin-dependent inflammatory network. *Cell* **133**, 1019-1031. doi:10.1016/j.cell.2008.03.039

Kurzrock, R., Hickish, T., Wyrwicz, L., Saunders, M., Wu, Q., Stecher, M., Mohanty, P., Dinarello, C. A. and Simard, J. (2019). Interleukin-1 receptor antagonist levels predict favorable outcome after bermekimab, a first-in-class true human interleukin-1α antibody, in a phase III randomized study of advanced colorectal cancer. *Oncoimmunology* **8**, 1551651. doi:10.1080/2162402X.2018.1551651

La, E., Rundhaug, J. E. and Fischer, S. M. (2001). Role of intracellular interleukin-1 receptor antagonist in skin carcinogenesis. *Mol. Carcinog.* **30**, 218-223. doi:10.1002/mc.1031

Lallemant, B., Evrard, A., Combescure, C., Chapuis, H., Chambon, G., Raynal, C., Reynaud, C., Sabra, O., Joubert, D., Hollande, F. et al. (2009). Clinical relevance of nine transcriptional molecular markers for the diagnosis of head and neck squamous cell carcinoma in tissue and saliva rinse. *BMC Cancer* **9**, 370. doi:10.1186/1471-2407-9-370

Lau, L., Porciuncula, A., Yu, A., Iwakura, Y. and David, G. (2019). Uncoupling the senescence-associated secretory phenotype from cell cycle exit via interleukin-1 inactivation unveils its protumorigenic role. *Mol. Cell. Biol.* **39**, e00586-18. doi:10.1128/MCB.00586-18

Leethanakul, C., Patel, V., Gillespie, J., Shillitoe, E., Kellman, R. M., Ensley, J. F., Limwongse, V., Emmert-Buck, M. R., Krizman, D. B. and Gutkind, J. S. (2000). Gene expression profiles in squamous cell carcinomas of the oral cavity: use of laser capture microdissection for the construction and analysis of stage-specific cDNA libraries. *Oral Oncol.* **36**, 474-483. doi:10.1016/S1368-8375(00)00039-7

Leung, E. Y., Mcmahon, J. D., Mclellan, D. R., Syyed, N., Mccarthy, C. E., Nixon, C., Orange, C., Brock, C., Hunter, K. D. and Adams, P. D. (2017). DNA damage marker phosphorylated histone H2AX is a potential predictive marker for

progression of epithelial dysplasia of the oral cavity. *Histopathology* **71**, 522-528. doi:10.1111/his.13260

Lewis, A. M., Varghese, S., Xu, H. and Alexander, H. R. (2006). Interleukin-1 and cancer progression: the emerging role of interleukin-1 receptor antagonist as a novel therapeutic agent in cancer treatment. *J. Transl. Med.* **4**, 48. doi:10.1186/1479-5876-4-48

Loaiza, N. and Demaria, M. (2016). Cellular senescence and tumor promotion: is aging the key? *Biochim. Biophys. Acta* **1865**, 155-167. doi:10.1016/j.bbcan.2016.01.007

Lodi, G., Franchini, R., Warnakulasuriya, S., Varoni, E. M., Sardella, A., Kerr, A. R., Carrassi, A., MacDonald, L. C. and Worthington, H. V. (2016). Interventions for treating oral leukoplakia to prevent oral cancer. *Cochrane Database Syst. Rev.* **7**, CD001829. doi:10.1002/14651858.CD001829.pub4

Malaquin, N., Vercamer, C., Bouali, F., Martien, S., Deruy, E., Wernert, N., Chwastyniak, M., Pinet, F., Abbadie, C. and Pourtier, A. (2013). Senescent fibroblasts enhance early skin carcinogenic events via a paracrine MMP-PAR-1 axis. *PLoS ONE* **8**, e63607. doi:10.1371/journal.pone.0063607

Malyak, M., Guthridge, J. M., Hance, K. R., Dower, S. K., Freed, J. H. and Arend, W. P. (1998a). Characterization of a low molecular weight isoform of IL-1 receptor antagonist. *J. Immunol.* **161**, 1997-2003.

Malyak, M., Smith, M. F., Jr., Abel, A. A., Hance, K. R. and Arend, W. P. (1998b). The differential production of three forms of IL-1 receptor antagonist by human neutrophils and monocytes. *J. Immunol.* **161**, 2004-2010.

Marur, S. and Forastiere, A. A. (2016). Head and neck squamous cell carcinoma: update on epidemiology, diagnosis, and treatment. *Mayo Clin. Proc.* **91**, 386-396. doi:10.1016/j.mayocp.2015.12.017

McGregor, F., Wagner, E., Felix, D., Soutar, D., Parkinson, K. and Harrison, P. R. (1997). Inappropriate retinoic acid receptor-beta expression in oral dysplasias: correlation with acquisition of the immortal phenotype. *Cancer Res.* **57**, 3886-3889.

McGregor, F., Muntoni, A., Fleming, J., Brown, J., Felix, D. H., Macdonald, D. G., Parkinson, E. K. and Harrison, P. R. (2002). Molecular changes associated with oral dysplasia progression and acquisition of immortality: potential for its reversal by 5-azacytidine. *Cancer Res.* **62**, 4757-4766.

Merhi-Soussi, F., Berti, M., Wehrle-Haller, B. and Gabay, C. (2005). Intracellular interleukin-1 receptor antagonist type 1 antagonizes the stimulatory effect of interleukin-1α precursor on cell motility. *Cytokine* **32**, 163-170. doi:10.1016/j.cyto.2005.09.004

Napier, S. S. and Speight, P. M. (2008). Natural history of potentially malignant oral lesions and conditions: an overview of the literature. *J. Oral Pathol. Med.* **37**, 1-10. doi:10.1111/j.1600-0714.2007.00579.x

Natarajan, E., Saeb, M., Crum, C. P., Woo, S. B., Mckee, P. H. and Rheinwald, J. G. (2003). Co-expression of p16(INK4A) and laminin 5 gamma2 by microinvasive and superficial squamous cell carcinomas in vivo and by migrating wound and senescent keratinocytes in culture. *Am. J. Pathol.* **163**, 477-491. doi:10.1016/S0002-9440(10)63677-2

Natarajan, E., Omobono, J. D., II, Guo, Z., Hopkinson, S., Lazar, A. J. F., Brenn, T., Jones, J. C. and Rheinwald, J. G. (2006). A keratinocyte hypermotility/growth-arrest response involving laminin 5 and p16INK4A activated in wound healing and senescence. *Am. J. Pathol.* **168**, 1821-1837. doi:10.2353/ajpath.2006.051027

Orjalo, A. V., Bhaumik, D., Gengler, B. K., Scott, G. K. and Campisi, J. (2009). Cell surface-bound IL-1α is an upstream regulator of the senescence-associated IL-6/IL-8 cytokine network. *Proc. Natl. Acad. Sci. USA* **106**, 17031-17036. doi:10.1073/pnas.0905299106

Ortiz-Montero, P., Londoño-Vallejo, A. and Vernot, J.-P. (2017). Senescence-associated IL-6 and IL-8 cytokines induce a self- and cross-reinforced senescence/inflammatory milieu strengthening tumorigenic capabilities in the MCF-7 breast cancer cell line. *Cell Commun. Signal.* **15**, 17. doi:10.1186/s12964-017-0172-3

Palmer, G., Trolliet, S., Talabot-Ayer, D., Mezin, F., Magne, D. and Gabay, C. (2005). Pre-interleukin-1α expression reduces cell growth and increases interleukin-6 production in SaOS-2 osteosarcoma cells: differential inhibitory effect of interleukin-1 receptor antagonist (icIL-1Ra1). *Cytokine* **31**, 153-160. doi:10.1016/j.cyto.2005.03.007

Rheinwald, J. G. and Green, H. (1975). Serial cultivation of strains of human epidermal keratinocytes: the formation of keratinizing colonies from single cells. *Cell* **6**, 331-343. doi:10.1016/S0092-8674(75)80001-8

Rheinwald, J. G., Hahn, W. C., Ramsey, M. R., Wu, J. Y., Guo, Z., Tsao, H., de Luca, M., Catricalà, C. and O'toole, K. M. (2002). A two-stage, p16INK4A- and

p53-dependent keratinocyte senescence mechanism that limits replicative potential independent of telomere status. *Mol. Cell. Biol.* **22**, 5157-5172. doi:10.1128/MCB.22.14.5157-5172.2002

Rovillain, E., Mansfield, L., Caetano, C., Alvarez-Fernandez, M., Caballero, O. L., Medema, R. H., Hummerich, H. and Jat, P. S. (2011). Activation of nuclear factor-kappa B signalling promotes cellular senescence. *Oncogene* **30**, 2356-2366. doi:10.1038/onc.2010.611

Schmalbach, C. E., Chepeha, D. B., Giordano, T. J., Rubin, M. A., Teknos, T. N., Bradford, C. R., Wolf, G. T., Kuick, R., Misek, D. E., Trask, D. K. et al. (2004). Molecular profiling and the identification of genes associated with metastatic oral cavity/pharynx squamous cell carcinoma. *Arch. Otolaryngol. Head Neck Surg.* **130**, 295-302. doi:10.1001/archotol.130.3.295

Shiiba, M., Saito, K., Yamagami, H., Nakashima, D., Higo, M., Kasamatsu, A., Sakamoto, Y., Ogawara, K., Uzawa, K., Takiguchi, Y. et al. (2015). Interleukin-1 receptor antagonist (IL1RN) is associated with suppression of early carcinogenic events in human oral malignancies. *Int. J. Oncol.* **46**, 1978-1984. doi:10.3892/ijo.2015.2917

Sparmann, A. and Bar-Sagi, D. (2004). Ras-induced interleukin-8 expression plays a critical role in tumor growth and angiogenesis. *Cancer Cell* **6**, 447-458. doi:10.1016/j.ccr.2004.09.028

Tomo, S., Biss, S. P., Crivelini, M. M., de Oliveira, S. H. P., Biasoli, E. R., Tjioe, K. C., Bernabe, D. G., Villa, L. L. and Miyahara, G. I. (2020). High p16(INK4a) immunoexpression is not HPV dependent in oral leukoplakia. *Arch. Oral Biol.* **115**, 104738. doi:10.1016/j.archoralbio.2020.104738

Uekawa, N., Nishikimi, A., Isobe, K.-I., Iwakura, Y. and Maruyama, M. (2004). Involvement of IL-1 family proteins in p38 linked cellular senescence of mouse embryonic fibroblasts. *FEBS Lett.* **575**, 30-34. doi:10.1016/j.febslet.2004.08.033

Villa, A., Celentano, A., Glurich, I., Borgnakke, W. S., Jensen, S. B., Peterson, D. E., Delli, K., Ojeda, D., Vissink, A. and Farah, C. S. (2019). World Workshop on Oral Medicine VII: prognostic biomarkers in oral leukoplakia: a systematic review of longitudinal studies. *Oral Dis.* **25** Suppl. 1, 64-78. doi:10.1111/odi.13087

Vincent, J., Adura, C., Gao, P., Luz, A., Lama, L., Asano, Y., Okamoto, R., Imaeda, T., Aida, J., Rothamel, K. et al. (2017). Small molecule inhibition of cGAS reduces interferon expression in primary macrophages from autoimmune mice. *Nat. Commun.* **8**, 750. doi:10.1038/s41467-017-00833-9

von Biberstein, S. E., Spiro, J. D., Lindquist, R. and Kreutzer, D. L. (1996). Interleukin-1 receptor antagonist in head and neck squamous cell carcinoma. *Arch. Otolaryngol. Head Neck Surg.* **122**, 751-759. doi:10.1001/archotol.1996.01890190047012

Weissbach, L., Tran, K., Colquhoun, S. A., Champliaud, M.-F. and Towle, C. A. (1998). Detection of an interleukin-1 intracellular receptor antagonist mRNA variant. *Biochem. Biophys. Res. Commun.* **244**, 91-95. doi:10.1006/bbrc.1998.8217

Werman, A., Werman-Venkert, R., White, R., Lee, J.-K., Werman, B., Krelin, Y., Voronov, E., Dinarello, C. A. and Apte, R. N. (2004). The precursor form of IL-1α is an intracrine proinflammatory activator of transcription. *Proc. Natl. Acad. Sci. USA* **101**, 2434-2439. doi:10.1073/pnas.0308705101

Whipple, M. E., Mendez, E., Farwell, D. G., Agoff, S. N. and Chen, C. (2004). A genomic predictor of oral squamous cell carcinoma. *Laryngoscope* **114**, 1346-1354. doi:10.1097/00005537-200408000-00006

Wiggins, K. A., Parry, A. J., Cassidy, L. D., Humphry, M., Webster, S. J., Goodall, J. C., Narita, M. and Clarke, M. C. H. (2019). IL-1α cleavage by inflammatory caspases of the noncanonical inflammasome controls the senescence-associated secretory phenotype. *Aging Cell* **18**, e12946. doi:10.1111/acel.12946

Wolf, J. S., Chen, Z., Dong, G., Sunwoo, J. B., Bancroft, C. C., Capo, D. E., Yeh, N. T., Mukaida, N. and VAN Waes, C. (2001). IL (Interleukin)-1 promotes Nuclear Factor-κB and AP-1-induced IL-8 expression, cell survival, and proliferation in head and neck squamous cell carcinomas. *Clin. Cancer Res.* **7**, 1812-1820.

Wu, S., Hu, G., Chen, J. and Xie, G. (2014). Interleukin 1β and interleukin 1 receptor antagonist gene polymorphisms and cervical cancer: a meta-analysis. *Int. J. Gynecol. Cancer* **24**, 984-990. doi:10.1097/IGC.0000000000000165

Wu, T., Hong, Y., Jia, L., Wu, J., Xia, J., Wang, J., Hu, Q. and Cheng, B. (2016). Modulation of IL-1β reprogrammes the tumor microenvironment to interrupt oral carcinogenesis. *Sci. Rep.* **6**, 20208. doi:10.1038/srep20208

Zhang, Y., Liu, C., Peng, H., Zhang, J. and Feng, Q. (2012). IL1 receptor antagonist gene IL1-RN variable number of tandem repeats polymorphism and cancer risk: a literature review and meta-analysis. *PLoS ONE* **7**, e46017. doi:10.1371/journal.pone.0046017